DOI: 10.1002/ejic.200800529

Heterometallic Transition-Metal Complexes Based on 1-Carboxy-1′-(diphenylphosphanyl)ferrocene, (tmeda/pmdta)Zinc(II), and Gold(I) Units

Janett Kühnert,[a] Petra Ecorchard,[a] and Heinrich Lang*[a]

Keywords: Heteromultimetallic complexes / Transition metals / Acetylides / Ferrocene / Cyclic voltammetry

The synthesis of the Zn^{II} and Ti^{IV} carboxylates [$L_nM(O_2CfcPPh_2)_2$] {L_nM = (tmeda)Zn (**3**); L_nM = (pmdta)Zn (**8**); L_nM = [Ti] (**12**); fc = $(\eta^5\text{-}C_5H_4)_2Fe$; tmeda = *N*,*N*,*N*′,*N*′-*tetra*methylethylene*dia*mine; pmdta = 1,1,4,7,7-*penta*methyl-*di*ethylen*tria*mine; [Ti] = $(\eta^5\text{-}C_5H_5)_2Ti$} and [$L_nM(X)(O_2C$-$fcPPh_2)$] {$L_nM$ = (pmdta)Zn, X = Cl (**7**); L_nM = [Ti], X = Me (**10**)} is reported. The reaction of Hdpf (**1**) {Hdpf = $(\eta^5\text{-}C_5H_4CO_2H)(\eta^5\text{-}C_5H_4PPh_2)Fe$} with [(tht)AuCl] (**13**) (tht = *tetra*hydro*th*iophene) gave [(Hdpf)AuCl] (**14**). Treatment of **3**, **7**, and **10** with **13** produced trimetallic [$L_nM(X)\{(O_2CfcPPh_2)$-AuCl}] {L_nM = [Ti], X = Me (**15**); L_nM = (pmdta)Zn, X = Cl (**16**)} or [(tmeda)Zn{$(O_2CfcPPh_2)AuCl\}_2$] (**17**). Heptametallic complexes were accessible by the reaction of **14** with HC≡CR {R = Fc, Rc; Fc = $(\eta^5\text{-}C_5H_4)(\eta^5\text{-}C_5H_5)Fe$; Rc = $(\eta^5\text{-}C_5H_4)(\eta^5\text{-}C_5H_5)Ru$}, whereby [$(H_2NEt_2)\{(O_2CfcPPh_2)AuCl\}$] (**18**) and [$(H_2NEt_2)\{(O_2CfcPPh_2)AuC{\equiv}CR\}$] {R = Fc (**20a**), Rc (**20b**)} were formed. Further reaction of **20a** and **20b** with [(tmeda)$ZnCl_2$] (**2**) gave [(tmeda)Zn{$(O_2CfcPPh_2)AuC{\equiv}CR\}_2$] {R = Fc (**21a**), Rc (**21b**)}. The solid-state structures of **3**, **7**, **12**, and **18** were determined by single-crystal X-ray diffraction. The Zn atom in **3** is in a distorted tetrahedral environment, while in **7** it is part of a distorted bipyramidal arrangement. In **18**, a stairlike 1D chain is built from three independent molecules of **18** by N–H···O hydrogen bonds and π–π interactions between phenyl or cyclopentadienyl rings of adjacent molecules. The cyclovoltammetric properties of **3**, **7**, **14**, **16**, **17**, **18**, **21a**, and **21b** are reported.

Introduction

The synthesis of hetero(multi)metallic molecules in which different early and late transition metals are linked by organic and/or inorganic units became increasingly of interest during the last years,[1] since these compounds offer unique structural features, novel chemical and physical properties, and they may provide cooperative effects between the different metal atoms.[2]

Owing to their redox chemistry, chemical robustness, and synthetic versatility, ferrocenyl building blocks have attracted significant attention as excellent donor groups in transition-metal chemistry. For example, carboxyl, phosphane, or alkynyl-functionalized ferrocenes offer the possibility to function as precursors for the synthesis of hetero(multi)metallic complexes.[3] Other preferred organometallic groups to be incorporated in complexes of higher nuclearity are phosphanylgold(I) chlorides, [$(R_3P)AuCl$], or -acetylides, [$(R_3P)AuC{\equiv}CR$] (R = single-bonded organic or organometallic group), because these species can be used for further functionalization and for the preparation of metal–organic or organometallic complexes of higher nuclearity. Moreover, gold(I) acetylides possess strong metal–carbon bonds, which makes them attractive molecules for many applications in material sciences.[1e,1j,4]

Titanium(IV) and zinc(II) ferrocenylcarboxylates are well-known; however, these systems are generally limited to the preparation of heterodimetallic compounds.[5] Their availability in hetero(multi)metallic complexes is not common, even though they may provide interesting structural features due to versatile coordination modes of the carboxyl unit,[5d] giving rise to the capability to form manifold unique structures.[5e]

Hetero(multi)metallic compounds containing organometallic fragments are common; however, the combination of organometallic and metal–organic building blocks in molecules of higher nuclearity are rare.[6] This prompted us to use 1-(carboxylic acid)-1′-(diphenylphosphanyl)ferrocene (Hdpf) as connecting unit for such building blocks, because the PPh_2 group preferentially coordinates to, for example, gold(I) moieties, whereas the carboxyl functionality in Hdpf enables the binding of zinc(II) and titanium(IV) fragments.

With respect to this background, we here report on the use of different synthesis methodologies for the preparation of hetero(multi)nuclear transition-metal complexes in which organometallic fragments are combined with metal–organic units based on zinc(II) and titanium(IV) carboxylates. The

[a] Technische Universität Chemnitz, Fakultät für Naturwissenschaften, Institut für Chemie, Lehrstuhl für Anorganische Chemie,
Straße der Nationen 62, 09111 Chemnitz, Germany
E-mail: heinrich.lang@chemie.tu-chemnitz.de

reaction chemistry, reactivity, structure, and bonding of these compounds is discussed. The electrochemical behavior of selected samples is described as well.

Results and Discussion

The zinc(II) carboxylate [(tmeda)Zn(O_2CfcPPh_2)$_2$] (**3**) [fc = ferrocene-1,1′-diyl, (η^5-C_5H_4)$_2$Fe; tmeda = *N*,*N*,*N*′,*N*′-*t*etra*m*ethyl*e*thylene*d*i*a*mine], in which two 1-carboxy-1′-(diphenylphosphanyl)ferrocene sandwich fragments are bridged by a metal–organic [(tmeda)Zn] unit could be synthesized by the following reactions: treatment of Hdpf (**1**) [Hdpf = (η^5-$C_5H_4CO_2H$)(η^5-$C_5H_4PPh_2$)Fe] with triethylamine in methanol gave the ammonium salt [$HNEt_3$](O_2CfcPPh_2), which further reacted with [(tmeda)Zn(NO_3)$_2$] (**5**), generated in situ from [(tmeda)ZnCl_2] (**2**) and [$AgNO_3$], to produce **3**. Since [$HNEt_3$]NO_3, formed concomitantly in the reaction of **1** with **2**, has a similar solubility as **3**, it was not possible to separate this material from complex **3**. Therefore, an alternative synthesis method had to be developed, which used NaOH for the deprotonation of **1** and **2** as zinc source. This allowed the successful isolation of **3** in analytically pure form and good yield [Equation (1), Experimental Section].

In a similar manner [(pmdta)Zn(Cl)(O_2CfcPPh_2)] (**7**) and [(pmdta)Zn(O_2CfcPPh_2)$_2$] (**8**) (pmdta = 1,1,4,7,7-*p*enta*m*ethyl*d*iethylen*t*ri*a*mine) could be prepared depending on the stoichiometry of the reactants used. Nevertheless, the reaction of **1** with **5** did not give [(pmdta)Zn(NO_3)(O_2CfcPPh_2)] (**6**). In this case, only **8** together with **5** could be isolated (Scheme 1).

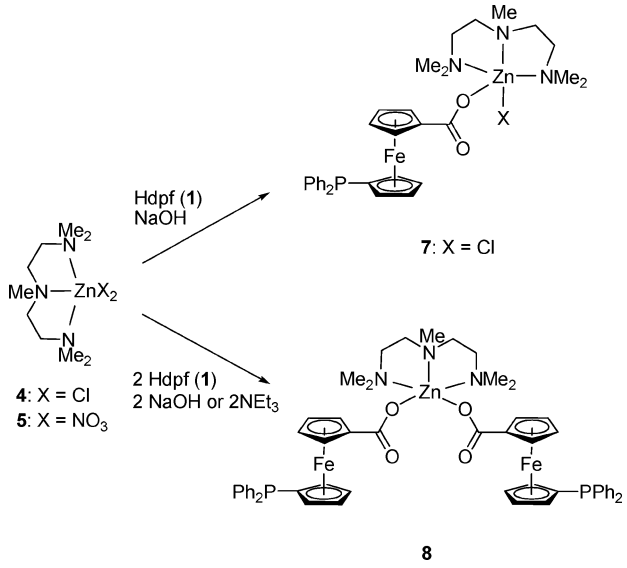

Scheme 1. Synthesis of **7** and **8** from **4** and **5**.

A possibility to introduce a titanocene fragment as a terminal as well as a connecting unit is presented in Scheme 2. Treatment of **1** with stoichiometric amounts of [Ti]Me_2 (**9**) {[Ti] = (η^5-C_5H_5)$_2$Ti} afforded heterodimetallic [Ti](Me)(O_2CfcPPh_2) (**10**), which, after appropriate work-up, could be isolated in quantitative yield (Experimental Section).

When **1** and **9** were reacted in a 2:1 stoichiometry, the expected dicarboxylate complex [Ti](O_2CfcPPh_2)$_2$ (**12**), in which the [Ti] building block connects two (η^5-$C_5H_4PPh_2$)(η^5-$C_5H_4CO_2$)Fe units, was formed in 30% yield (Experimental Section). The use of different reaction conditions (excess **1**, higher temperature, longer reaction time) did not give higher amounts of **12**. However, the best method to synthesize **12** is the reaction of [Ti]Cl_2 (**11**) with **1** in a 1:2 molar ratio in the presence of triethylamine (Scheme 2).

Ferrocenes **1**, **7**, and **10**, with the Ph_2P unit, possess a P-ligating site which enables the introduction of additional organometallic and/or metal–organic fragments. For example, we treated **1**, **7**, and **10** with one equivalent of [(tht)AuCl] (**13**) (tht = *t*etra*h*ydro*t*hiophene). Substitution of tht by the stronger Lewis base XO_2CfcPPh_2 {X = H, (pmdta)ZnCl, [Ti]Me} produced complexes **14**–**16**, which, after appropriate work-up, could be isolated as pale orange (**14**) or pale yellow (**15**, **16**) solids [Equation (2)].

Under similar reaction conditions, complex **3** containing two 1-carboxy-1′-(diphenylphosphanyl)ferrocene units reacted with **13** in a 1:2 stoichiometry to afford pentametallic Fe_2Au_2Zn complex **17** [Equation (3)].

Molecules **14**–**17**, with their terminal AuCl entities, are predestined for the synthesis of transition-metal complexes with higher nuclearity. Heptametallic **21a** and **21b**, featuring three (Fe, Au, Zn) or even four (Fe, Au, Zn, Ru) different transition-metal atoms, are accessible by the synthesis protocol shown in Scheme 3. In these molecules, two organometallic (O_2CfcPPh_2)AuC≡CR moieties (R = Fc, Rc) are connected by a metal–organic [Zn(tmeda)] bridging unit.

Molecules **21a** and **21b** could be prepared in a consecutive way by starting from **14**. Treatment of this sandwich compound with $HNEt_2$ produced ionic [(H_2NEt_2)-{(O_2CfcPPh_2)AuCl}] (**18**), which further reacted with

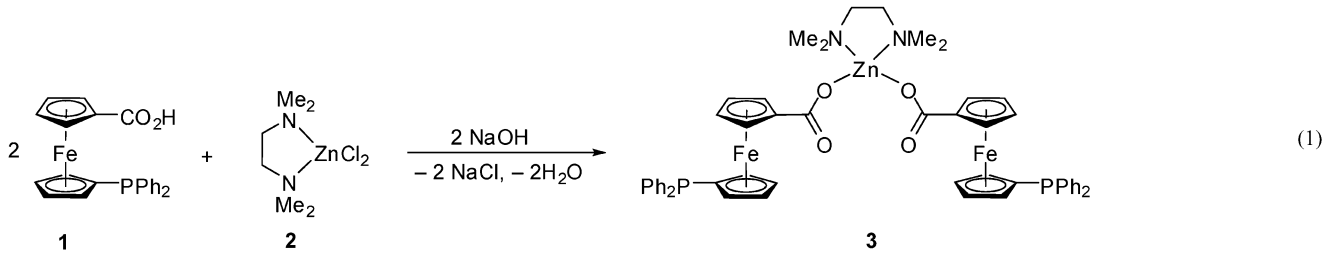

(1)

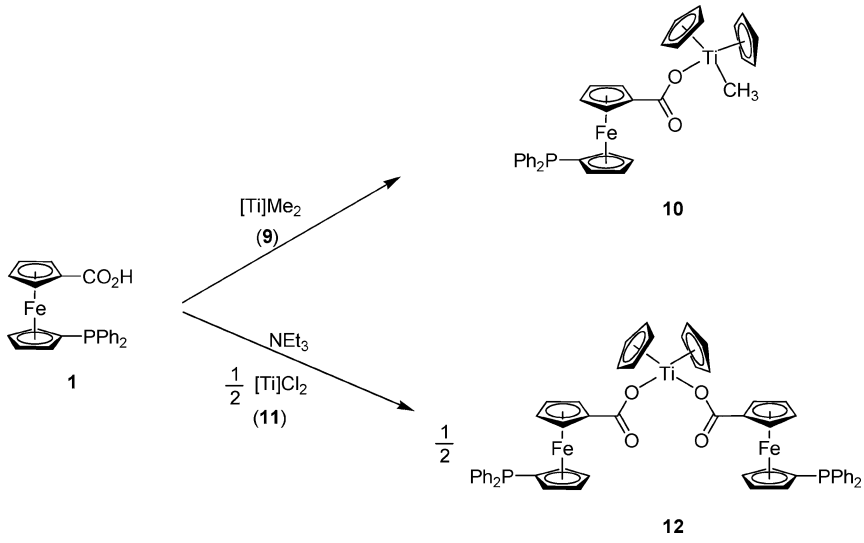

Scheme 2. Synthesis of **10** and **12**.

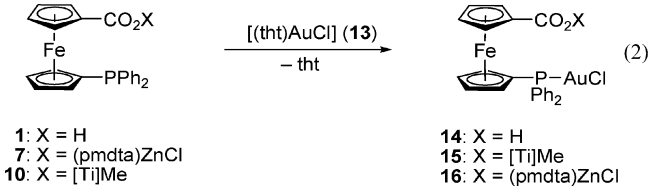

HC≡CR {R = Fc (**19a**); R = Rc (**19b**)} to give [(H_2NEt_2){$(O_2CfcPPh_2)AuC{\equiv}CR$}] {R = Fc (**20a**); R = Rc (**20b**); Fc = (η^5-C_5H_4)(η^5-C_5H_5)Fe, Rc = (η^5-C_5H_4)(η^5-C_5H_5)Ru} (Scheme 3). Unfortunately, **20a** and **20b** show the same solubility behavior as **19a** and **19b**, and hence these molecules could not be separated from each other either by chromatography or by crystallization. Acidification of **20a** and **20b** resulted in the decomposition of these molecules. For this reason, we treated the corresponding mixtures [H_2NEt_2]Cl/**20a** and [H_2NEt_2]Cl/**20b**, as obtained in the reaction of **18** with **19**, directly with **2** in the molar ratio of 2:1 in methanol. As a result of these reactions, complexes **21a** and **21b** precipitated as pale orange or pale yellow solids, respectively.

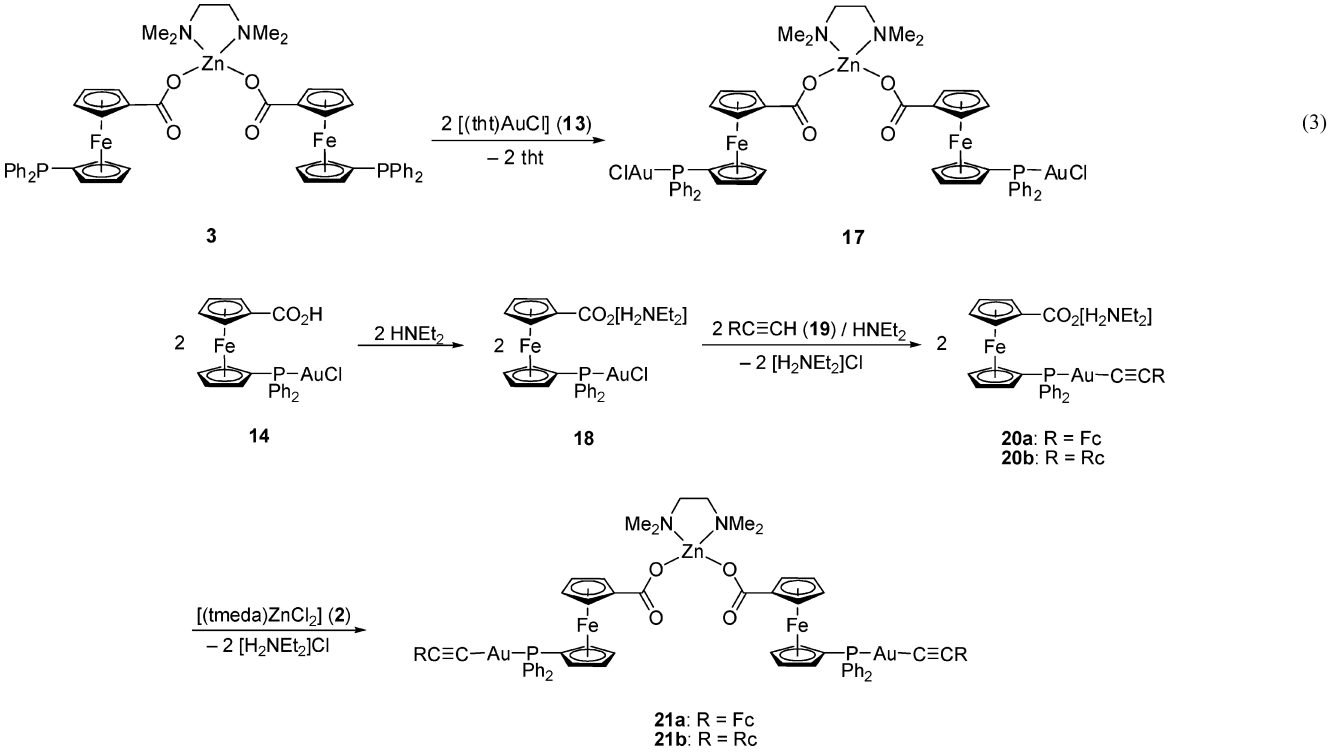

Scheme 3. Synthesis of heptametallic **21a** and **21b** [Fc = (η^5-C_5H_4)(η^5-C_5H_5)Fe, Rc = (η^5-C_5H_4)(η^5-C_5H_5)Ru].

Compounds **3**, **7**, **8**, **12**, **14**, **16**–**18**, **20**, and **21** are stable in the solid state and dissolve in organic solvents including dichloromethane and tetrahydrofuran. An exception is heterodimetallic **10**, which rapidly decomposes in air. Even more reactive is **15**, which decomposes within minutes even at low temperature; hence, it could only be characterized by ESI-TOF mass spectrometric investigations.

All newly synthesized molecules were characterized by elemental analysis, IR and NMR spectroscopy (^{1}H, ^{13}C{^{1}H}, ^{31}P{^{1}H}), and ESI-TOF mass spectrometry, whereby the analytical and spectroscopic data confirm their composition as hetero(multi)metallic transition-metal complexes (Experimental Section).

Most informative for these molecules are their ^{31}P{^{1}H} NMR spectra. For molecules **3**, **7**, **8**, **10**, and **12**, resonance signals are observed at ca. –19 ppm, confirming the noncoordinating character of the PPh_2 moiety. Upon coordination to gold(I) chloride, as given in **14**, **16**, **17**, and **18**, a shift to ca. 27 ppm is typical. When the chloride ligand in **18** is replaced by the acetylide RC≡C {R = Fc (**21a**), Rc (**21b**)}, a further shift to lower field is observed (δ = 36 ppm).

The structures of **3** (Figure 1), **7** (Figure 2), **12** (Figure 3), and **18** (Figure 4 and Figure 5) in the solid state were determined by single-crystal X-ray diffraction. Relevant crystallographic and structural refinement data are summarized in Table 5 (Experimental Section). Representative bond lengths [Å] and angles [°] of **3** and **12** are given in the captions of Figure 1 and Figure 3, while for **7** and **18** these data are summarized in Table 1 and Table 2, respectively.

Single crystals were obtained by diffusion of *n*-hexane into a solution of the transition-metal complexes in a dichloromethane/methanol mixture (50:1, v/v) (**3**), dichloromethane (**7**), chloroform (**12**), or a dichloromethane/toluene mixture (10:1, v/v) (**18**) at room temperature. The molecules crystallize in the monoclinic space groups *P*2/*c* (for **3**), *C*2/*c* (for **12**), $P2_1/n$ (for **18**), or in the triclinic space group $P\bar{1}$ (for **7**). The asymmetric unit cell of **7** and **18** contains three

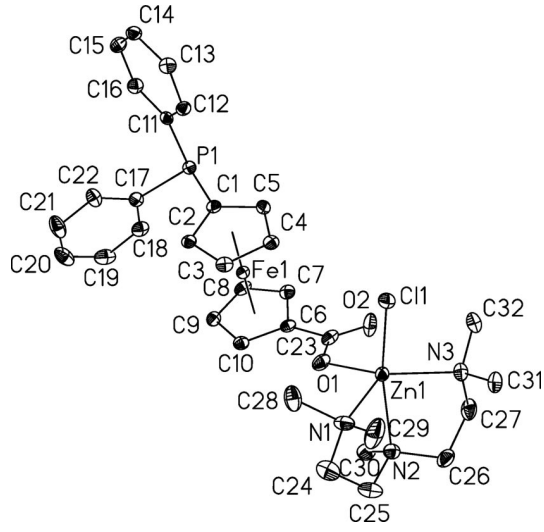

Figure 2. ORTEP diagram (30% probability level) of **7A** with the atom numbering scheme (the hydrogen atoms and the noncoordinating CH_2Cl_2 molecule are omitted for clarity). Selected bond lengths and angles of this molecule together with **7B** and **7C** are listed in Table 1.

crystallographically independent molecules. In **7** [(**7A** (Zn1), **7B** (Zn2), **7C** (Zn3)] these three molecules have similar bond lengths and angles (Table 1); therefore, only **7A** is discussed. In contrast, for **18** the three independent molecules [**18A** (Au1), **18B** (Au2), and **18C** (Au3)] show some differences in the rotation angles of their diphenylphosphanyl and carboxy substituents with respect to each other, as well as in the rotation angles of their cyclopentadienyl rings, most probably because of intermolecular contacts (vide infra). The cyclopentadienyl rings of the ferrocene units in **3**, **7**, **12**, and **18** exhibit an almost coplanar conformation, having dihedral angles of 1.9 (**3**), 5.2 (**7A**), 3.95 (**12**, fc with Fe1), 3.54 (**12**, fc with Fe2), 1.7 (**18A**), 2.6 (**18B**), and 2.7° (**18C**) between their calculated mean planes. An almost eclipsed conformation of the cyclopentadienyl rings of the

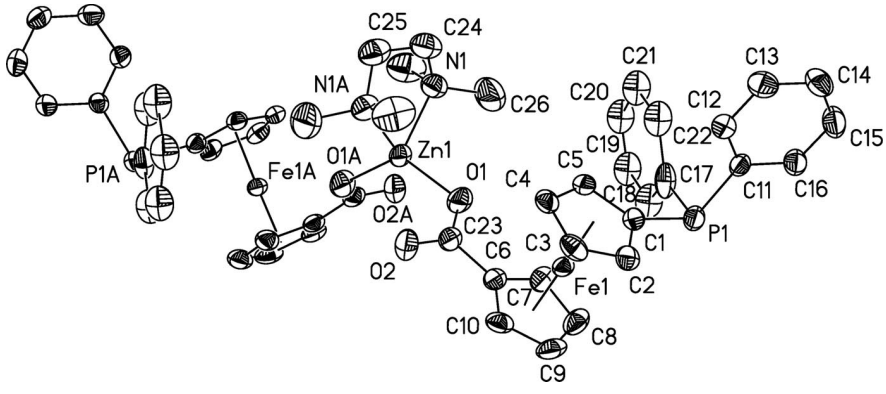

Figure 1. ORTEP diagram (30% probability level) of **3** with the atom numbering scheme (hydrogen atoms were omitted for clarity). Only one position of the disordered atoms (C18–C23) of the phenyl ring is shown. Atoms generated by the crystallographic symmetry operation (–*x*, *y*, –*z* + 3/2) by a C2 axis passing through Zn1 and the middle of C24–C24A are distinguished with the suffix A. Selected bond lengths [Å] and angles [°]: Zn1–N1 2.093(4), Zn1–O1 1.917(3), C23–O1 1.283(5), C23–O2 1.233(6), Fe1–D1 1.6418(18), Fe1–D2 1.6455(19); N1–Zn1–N1A 85.5(2), N1–Zn1–O1 104.56(16), N1A–Zn1–O1 118.92(15), O1–Zn1–O1A 119.9(2). (D1 = centroid of C1–C5, D2 = centroid of C6–C10). Standard uncertainties are given in the last significant figure(s) in parentheses.

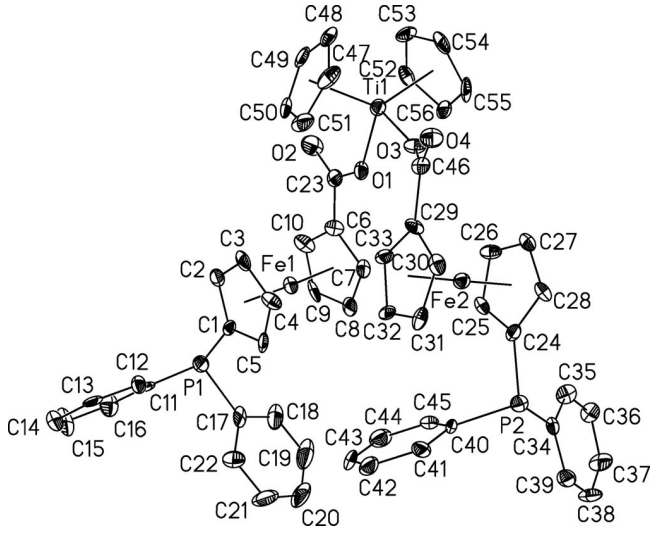

Figure 3. ORTEP diagram (50% probability level) of **12** with the atom numbering scheme (the hydrogen atoms are omitted for clarity). Selected bond lengths [Å] and angles [°]: Ti1–O1 1.989(3), Ti1–O3 1.896(3), Fe1–D1 1.6433(18), Fe1–D2 1.6435(18), Fe2–D3 1.6461(18), Fe2–D4 1.6489(19), Ti1–D5 2.0449(20), Ti1–D6 2.0571(19); C23–O1–Ti1 133.3(3), C46–O3–Ti1 152.2(3), O3–Ti1–O1 92.27(13). (D1 = centroid of C1–C5, D2 = centroid of C6–C10, D3 = centroid of C24–C28, D4 = centroid of C28–C33, D5 = centroid of C47–C51, D6 = centroid of C53–C56). Standard uncertainties are given in the last significant figure(s) in parentheses.

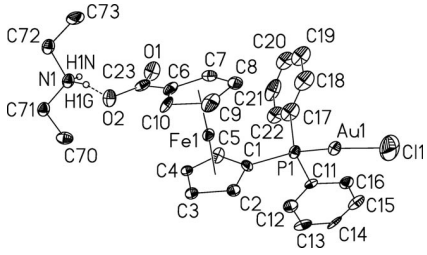

Figure 4. ORTEP diagram (50% probability level) of **18A** with the atom numbering scheme (hydrogen atoms, except H1G and H1N, are omitted for clarity). Selected bond lengths and angles of this molecule together with molecules **18B** and **18C** are given in Table 2.

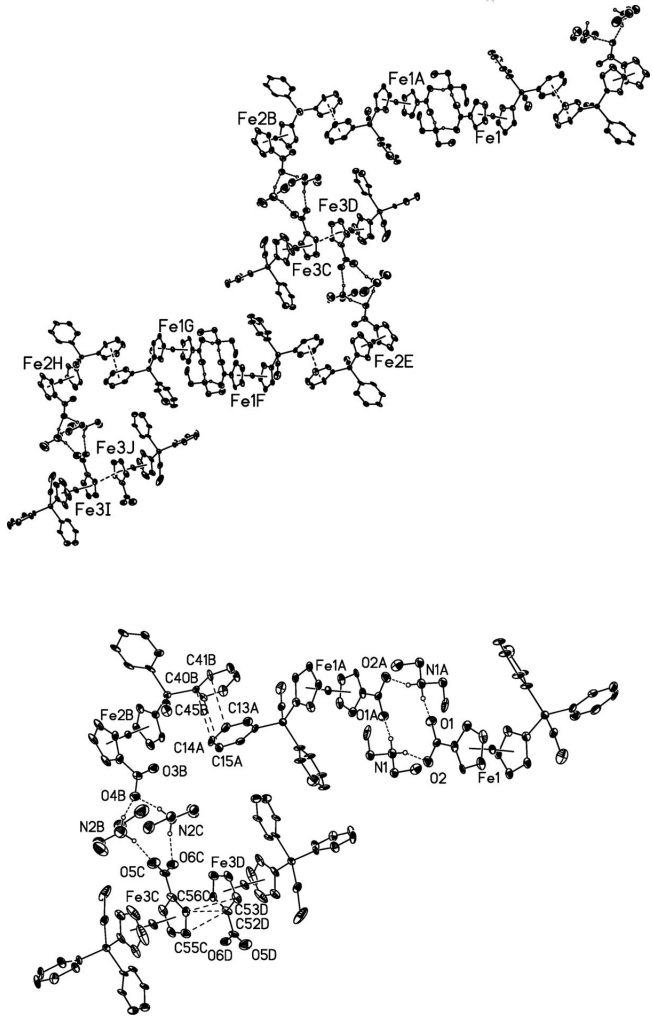

Figure 5. Selected parts of the 1D chain formed by complex **18** in the solid state induced by intermolecular hydrogen bonds and π–π interactions. Top: Elongated part of the 1D chain illustrating its stairlike arrangement. Bottom: Part of the 1D chain illustrating intermolecular interactions. Hydrogen atoms, except *N*-bonded hydrogen atoms are omitted for clarity. Labels A to J refer to symmetry-generated molecules.

ferrocenyl moieties in **7A**, **12**, **18A**, and **18B** is confirmed by rotation angles of 8.3 (**7A**), 5.48 (**12**, fc with Fe1), 11.8 (**18A**), and 13.3° (**18B**), while the rotation angles of 22.1 (**3**), 21.34 (**12**, fc with Fe2), and 27.8° (**18C**) verify an almost staggered confirmation, which is most likely attributed to steric hindrance. The torsion angles C1–D1–D2–C6 (123° for **3**, 152° for **7A**, 148° for **12**, fc with Fe1) and C24–D3–D4–C29 (165° for **12**, fc with Fe2) (D1, D3 = centroids of the $C_5H_4PPh_2$ cyclopentadienyl groups; D2, D4 = centroids of the $C_5H_4CO_2$ units) indicate that the substituents of the cyclopentadienyl rings are oriented in almost opposite directions. For the three independent molecules of **18** these torsion angles are significantly different [133° for **18A**, 86° for **18B**, 116° for **18C**] because of either steric effects or intermolecular contacts (vide infra).

In **3**, the metal center Zn1 is σ-bonded by one oxygen atom of the individual carboxyl functionalities and is additionally coordinated by the nitrogen atoms of the chelating tmeda ligand (Zn1–N1), which results in a distorted tetrahedral environment around Zn1 (Figure 1). The Zn1–N1 bond length is similar to the one found in [(tmeda)Zn(η^2-BH_4)(Cl)] {2.09(1) Å},[8] but it is somewhat shorter than that reported for octahedral [(tmeda)Zn($O_2CMe)_2$] {2.140(4) Å}.[9]

In contrast to **3**, where the zinc atom is tetrahedrally coordinated, in **7** it possesses a distorted trigonal-bipyramidal coordination sphere, having N1, N3, and O1 in equatorial and Cl1 and N2 in axial positions. The Zn1–N2 distance is found to be about 0.18 Å longer than that of the equatorial Zn1–N1 and Zn1–N3 separations. The bond lengths agree well with the values typical for pmdta-coordinated zinc complexes, e.g. [(pmdta)Zn(S_4)][10] and [(pmdta)Zn(Cl)-{$(OHC)_2CC_6H_4NO_2$}].[11]

Table 1. Selected bond lengths [Å] and angles [°] of the three independent molecules of **7** (**7A**, **7B**, and **7C**).[a]

7A (Zn1)		**7B** (Zn2)		**7C** (Zn3)	
Bond lengths					
O1–Zn1	1.977(3)	O3–Zn2	1.979(3)	O5–Zn3	1.979(3)
Zn1–N3	2.145(3)	Zn2–N4	2.150(3)	Zn3–N7	2.148(3)
Zn1–N1	2.147(3)	Zn2–N6	2.145(4)	Zn3–N9	2.149(4)
Zn1–N2	2.328(4)	Zn2–N5	2.330(3)	Zn3–N8	2.334(3)
Zn1–Cl1	2.3490(11)	Zn2–Cl2	2.3501(11)	Zn3–Cl3	2.3505(11)
Fe1–D1[b]	1.6384(17)	Fe2–D3[b]	1.6402(18)	Fe3–D5[b]	1.6404(17)
Fe1–D2[b]	1.6434(18)	Fe2–D4[b]	1.6437(18)	Fe3–D6[b]	1.6418(18)
Bond angles					
O1–Zn1–N3	132.38(13)	O3–Zn2–N4	132.58(13)	O5–Zn3–N7	132.58(13)
N3–Zn1–N1	127.84(14)	N4–Zn2–N6	127.80(14)	N7–Zn3–N9	127.76(14)
N1–Zn1–O1	94.82(14)	N6–Zn2–O3	94.75(14)	N9–Zn2–O5	94.79(14)
N2–Zn1–Cl1	165.57(9)	N5–Zn2–Cl2	165.67(9)	N8–Zn3–Cl3	165.57(9)
N2–Zn1–O1	89.87(12)	N5–Zn2–O3	89.84(12)	N8–Zn3–O5	89.99(12)

[a] Standard uncertainties are given in the last significant figure(s) in parentheses. [b] D1 = centroid of C1–C5, D2 = centroid of C6–C10, D3 = centroid of C33–C37, D4 = centroid of C38–C42, D5 = centroid of C65–C69, D6 = centroid of C79–C74.

Table 2. Selected bond lengths [Å] and angles [°] of the three independent molecules of **18** (**18A**, **18B**, and **18C**).[a]

18A (Fe1)		**18B** (Fe2)		**18C** (Fe3)	
Bond lengths					
C1–P1	1.806(15)	C24–P2	1.797(14)	C47–P3	1.793(15)
P1–Au1	2.222(4)	P2–Au2	2.225(4)	P3–Au3	2.230(4)
Au1–Cl1	2.292(4)	Au2–Cl2	2.292(4)	Au3–Cl3	2.287(5)
Fe1–D1[b]	1.637(7)	Fe2–D3[b]	1.637(7)	Fe3–D5[b]	1.640(8)
Fe1–D2[b]	1.658(7)	Fe2–D4[b]	1.634(7)	Fe3–D6[b]	1.660(7)
Bond angles					
P1–Au1–Cl1	174.13(16)	P2–Au2–Cl2	176.83(14)	P3–Au3–Cl3	176.00(18)
C1–P1–Au1	109.3(5)	C24–P2–Au2	119.9(5)	C47–P3–Au3	111.0(6)

[a] Standard uncertainties are given in the last significant figure(s) in parentheses. [b] D1 = centroid of C1–C5, D2 = centroid of C6–C10, D3 = centroid of C24–C28, D4 = centroid of C29–C33, D5 = centroid of C47–C51, D6 = centroid of C52–C56.

The titanium atom Ti1 in **12** possesses a distorted tetrahedral geometry. The titanium–oxygen (Ti1–O1, Ti1–O3) and titanium–cyclopentadienyl (Ti1–D5, Ti1–D6; D5, D6 = centroids of the C_5H_5 units) separations are in accordance with parameters reported for other titanium(IV) carboxylates, for example, $[Fe(CO)_2(CH_2Ph)\{(\eta^5\text{-}C_5H_4CO_2)[Ti]\}]$ $\{[Ti] = (\eta^5\text{-}C_5H_5)_2Ti\}$[5b] and $[(\eta^5\text{-}C_5H_4Me)_2Ti(O_2CPh)_2]$.[12] Both $O_2CfcPPh_2$ units are oriented opposite to each other. The P–P distance in **12** (P1–P2, 9.54 Å) is much shorter than that in **3** (P1–P1A, 15.07 Å), because of the different dihedral angles of the corresponding cyclopentadienyl and carboxyl planes (C6–C10 vs. C23/O1/O2, 9.65°; C29–C33 vs. C46/O3/O4, 25.08°) (Figure 3).

In heterodimetallic **18**, a linear arrangement at the gold atom is typical (Table 2). The bond lengths and angles of **18** agree well with those reported for similar phosphane-coordinated AuCl metal–organic complexes.[7,13]

The overall structural feature of the three independent molecules of **18** (**18A**, **18B**, and **18C**) in the solid state is that they form a stairlike 1D chain (Figure 5). The linking of individual molecules is supported by (Et_2NH)-H···O($OCfcPPh_2AuCl$) hydrogen bonds (Table 3) and π–π interactions (Figure 5). Motifs generated by hydrogen bonds can be described with the graph-set included by Etter.[14] Within the coordination polymer of **18**, two carboxyl units of individual molecules of **18A** are linked by two $[H_2NEt_2]^+$ moieties forming a 12-membered $C_2H_4N_2O_4$ cycle $[R_{44}(12)]$,[14] while each carboxyl functionality of **18B** and **18C** participates in two hydrogen bonds with two different $[H_2NEt_2]^+$ units, which results in a 10-membered $CH_4N_2O_3$ ring $[R_{34}(10)]$ (Table 3, Figure 5). The N···O separations of the (Et_2NH)H···O($OCfcPPh_2AuCl$) moieties are between 2.670(18) and 2.716(18) Å and can therefore be considered as medium-strong bonds.[15] These values are similar to intermolecular hydrogen bond lengths observed for $[Zn(diap)_2(OAc)_2]\cdot H_2O$ (diap = 1,3-*diaze*pane-2-thione), where a N···O separation of 2.792(2) Å is typical.[16] The H···O distance of the N–H···O bonds ranges from 1.75(14) to 1.80(12) Å [N–H···O angles, 155(11)–165(9)°] (Table 3).

Table 3. Selected bond lengths [Å] and angles [°] for intermolecular N–H···O hydrogen bonds of molecules **18A**, **18B**, and **18C**.[a]

N–H···O interaction	N–H	H···O	N···O	N–H···O angle
N1–H1G···O2	0.95(14)	1.75(14)	2.670(18)	161(11)
N1–H1N···O1	0.95(9)	1.77(8)	2.701(18)	164(10)
N2–H2G···O4	0.94(17)	1.80(14)	2.70(2)	158(14)
N2–H2N···O5	0.94(7)	1.77(8)	2.69(2)	165(9)
N3–H3G···O4	0.96(12)	1.78(15)	2.716(18)	165(14)
N3–H3N···O6	0.95(12)	1.80(12)	2.693(19)	155(11)

[a] Standard uncertainties are given in the last significant figure(s) in parentheses.

Between two phenyl rings of adjacent molecules of **18A** (C11–C16) and **18B** (C40–C45) there exist π–π interactions with an eclipsed sandwich configuration [*R*1 = 3.698 Å; *R*1 is the perpendicular distance of the center of C11–C16 (molecule **B**) to the ring C40–C45 (molecule **A**)].[17] The closest phenyl-C–H···C-phenyl distance is 3.672–3.720 Å, and the interplanar angle between neighboring phenyl rings is 4.6° (Figure 5). A second kind of π–π interaction is observed between two adjacent cyclopentadienyl groups of two individual molecules of **18C** showing a parallel displaced geometry [*R*1 = 3.333, *R*2 = 0.974 Å;[17] *R*1 is the perpendicular distance between the centers of C52–C56 in molecules **A** and **B**; *R*2 is the distance between the center of C52–C56 (molecule **A**) and the perpendicular projection of the center of C52–C56 in molecules **A** and **B**]. In this case, the closest Cp–C–H···C–Cp separations (Cp = C_5H_4 unit) are 3.348–3.493 Å. The interplanar angle between the adjacent cyclopentadienyl rings (C52–C56 of two different molecules of **18C**) is found to be 0° indicating perfect parallelism.

Complexes **3**, **7**, **14**, **16**, **17**, **18**, **21a**, and **21b** were subjected to cyclovoltammetric measurements. The electrochemical data are summarized in Table 4. The potentials

are given relative to the FcH/FcH$^+$ redox couple {FcH = (η^5-C_5H_5)$_2$Fe, E_0 = 0.00 V (ΔE_p = 0.10 V)}.[18] As representative examples, the cyclic voltammograms of **7**, **16**, **18**, and **21a** are presented in Figure 6, Figure 7, Figure 8, and Figure 9.

Table 4. Electrochemical data for **3**, **7**, **14**, **16**, and **17**.[a]

Compound	[Fe^{II}/Fe^{III}] $E_{p,ox}$ [V]	[Fe^{II}/Fe^{III}] E_0 (ΔE_p) [V]	[Au^I/Au^0] $E_{p,red}$ [V]
3	0.34	0.61 (0.105)	–
7	0.35	0.57 (0.130)	–
14	–	0.54 (0.075)	–
16	–	0.53 (0.120)	–2.56
17	–	0.49 (0.135)	–2.53

[a] Cyclic voltammograms from 5×10^{-4} M solutions in dichloromethane at 25 °C with [*n*-Bu$_4$N]PF$_6$ (0.1 M) as supporting electrolyte, scan rate = 0.10 V s^{-1}. All potentials are given in V and are referenced to the FcH/FcH$^+$ redox couple {FcH = (η^5-C_5H_5)$_2$Fe} with E_0 = 0.00 V (ΔE_p = 0.10 V).[18]

It is obvious that the electrochemical behavior for **3** and **7**, having a noncoordinated diphenylphosphanyl functionality, differs from the ones in which the diphenylphosphanyl group coordinates to a gold(I) moiety (**14**, **16**–**18**, **21**). The [Fe^{II}/Fe^{III}] redox potential of the (η^5-$C_5H_4CO_2$)(η^5-$C_5H_4PPh_2$)Fe units is thereby almost not influenced by the corresponding gold(I) moieties. Molecules **3** and **7** show, for their (diphenylphosphanyl)ferrocenyl building block, one irreversible oxidation peak followed by a reversible process (Figure 6, Table 4). The first irreversible oxidation is caused by the oxidation of Fe^{II}. The ferrocenium Fe^{III} system that is generated in this way is then reduced by an intramolecular electron transfer from the phosphane group to iron.[19] The resulting Fe^{II}–P^{IV} species is immediately stabilized by a further electrochemical oxidation of P^{IV} to P^V. A second independent electrochemical process involves the reversible [Fe^{II}/Fe^{III}] oxidation of the latter ferrocene–phosphane Fe^{II}–P^V species. Such behavior is typical for diphenylphosphanyl-substituted ferrocenes, for example, FcPPh$_2$ and

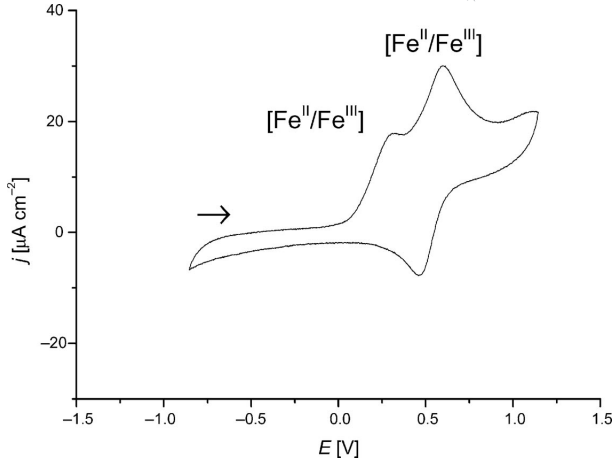

Figure 6. Cyclic voltammogram of **7** {5×10^{-4} M solution in dichloromethane at 25 °C with [*n*-Bu$_4$N]PF$_6$ (0.1 M) as supporting electrolyte, scan rate = 0.10 V s^{-1}}. All potentials are referenced to the FcH/FcH$^+$ redox couple {FcH = (η^5-C_5H_5)$_2$Fe} with E_0 = 0.00 V (ΔE_p = 0.10 V).[18]

HO$_2$CfcPPh$_2$ {Fc = (η^5-C_5H_4)(η^5-C_5H_5)Fe; fc = (η^5-C_5H_4)$_2$Fe}.[19]

Coordination of the PPh$_2$ group to a AuCl moiety, typical in **14**, **16**, and **17**, results in one reversible wave (Table 4, Figure 7) for the [Fe^{II}/Fe^{III}] redox couple, as the electron transfer (vide supra) from PPh$_2$ is prevented by the coordination of the PPh$_2$ group to gold(I). Only one wave for the [Fe^{II}/Fe^{III}] redox couple was found for **17**, where two Fe^{II} centers are present, indicating a simultaneous oxidation process for both Fe^{II} ions. The potentials of the [Fe^{II}/Fe^{III}] redox couples in **14**, **16**, and **17** indicate that they are not significantly affected by the carboxyl functionality. The reduction potential for gold(I) was observed at –2.56 V for **16** and at –2.53 V for **17** and is irreversible, i.e. no re-oxidation occurs.[7]

In contrast to **14**, ionic **18** shows a different electrochemical behavior, i.e. two different potentials for the [Fe^{II}/Fe^{III}]

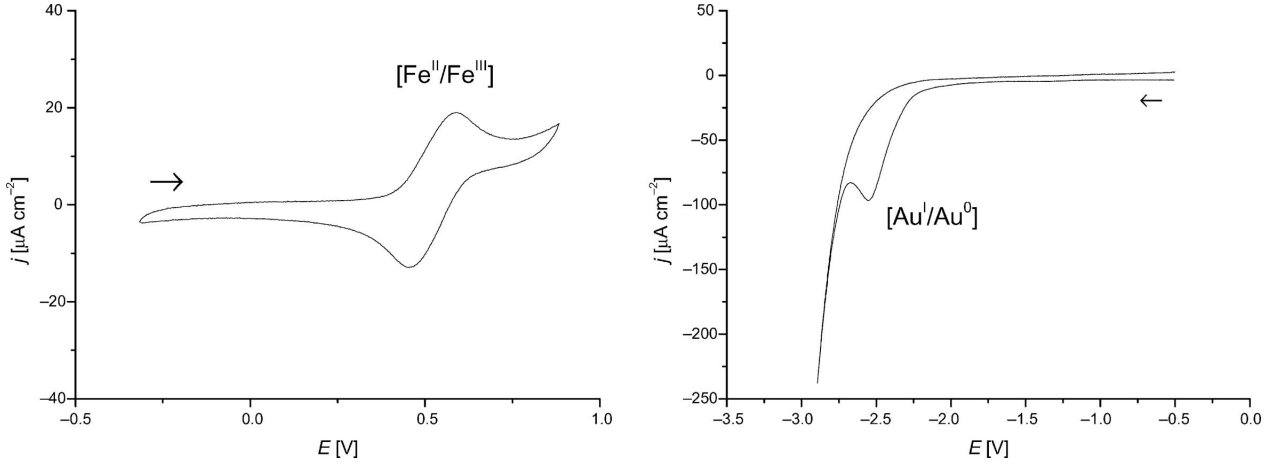

Figure 7. Cyclic voltammogram of **16** (left: [Fe^{II}/Fe^{III}] oxidation; right: [Au^I/Au^0] reduction) {5×10^{-4} M solution in dichloromethane at 25 °C with [*n*-Bu$_4$N]PF$_6$ (0.1 M) as supporting electrolyte, scan rate = 0.10 V s^{-1}}. All potentials are referenced to the FcH/FcH$^+$ redox couple {FcH = (η^5-C_5H_5)$_2$Fe} with E_0 = 0.00 V (ΔE_p = 0.10 V).[18]

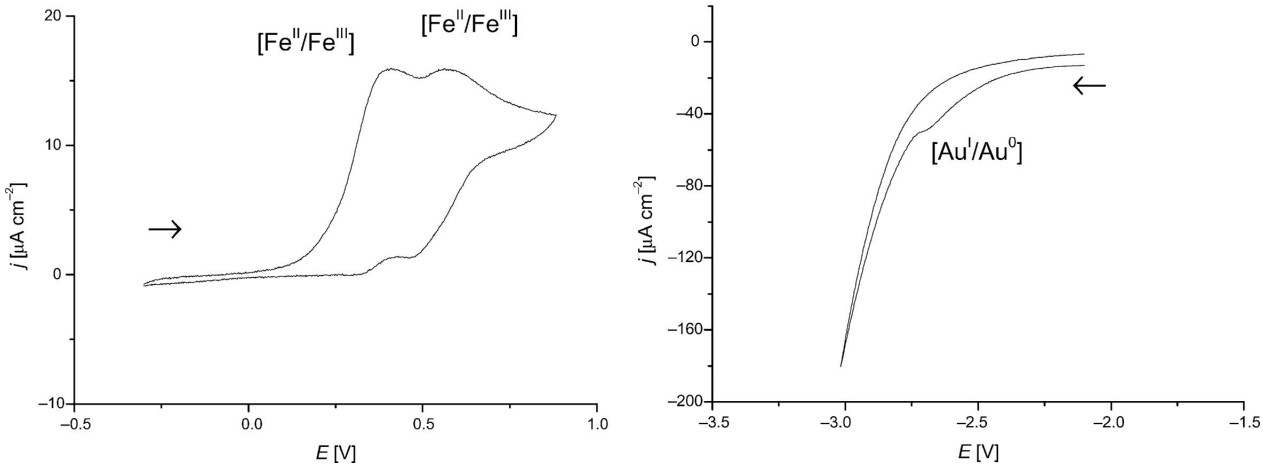

Figure 8. Cyclic voltammogram of **18** (left: [Fe^{II}/Fe^{III}] oxidation; right: [Au^{I}/Au^{0}] reduction) {5×10^{-4} M solution in dichloromethane at 25 °C with [*n*-Bu_4N]PF_6 (0.1 M) as supporting electrolyte, scan rate = 0.10 $V s^{-1}$}. All potentials are referenced to the FcH/FcH^+ redox couple {FcH = (η^5-$C_5H_5)_2Fe$} with E_0 = 0.00 V (ΔE_p = 0.10 V).[18]

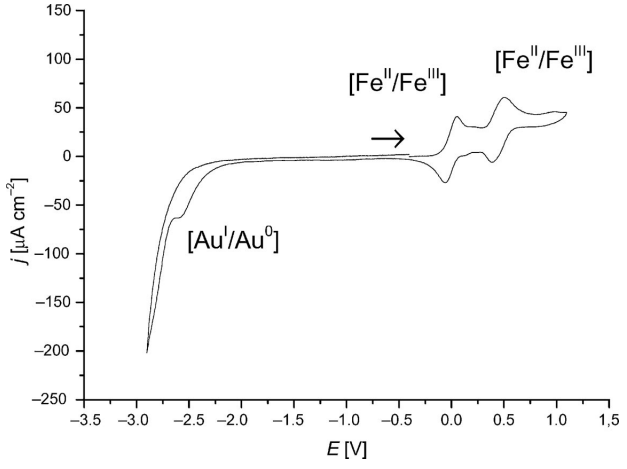

Figure 9. Cyclic voltammogram of **21a** {5×10^{-4} M solution in dichloromethane at 25 °C with [*n*-Bu_4N]PF_6 (0.1 M) as supporting electrolyte, scan rate = 0.10 $V s^{-1}$}. All potentials are referenced to the FcH/FcH^+ redox couple {FcH = (η^5-$C_5H_5)_2Fe$} with E_0 = 0.00 V (ΔE_p = 0.10 V).[18]

redox couple are observed at E_0 = 0.36 V (ΔE_p = 0.088 V) and E_0 = 0.53 V (ΔE_p = 0.094 V) (Figure 8). This is at first astonishing but most probably related to an equilibrium existing between the deprotonated [(H_2NEt_2){(O_2CfcPPh_2)-AuCl}] and protonated [(HO_2CfcPPh_2)AuCl] forms of **18**. Also the visibility of a reduction wave at E_0 = –1.6 V, which can be assigned to the CO_2H group, confirms this behavior. The same observation was made for $FcCO_2H$,[1a] which shows one reversible peak for the [Fe^{II}/Fe^{III}] redox couple, while for [(H_2NEt_2)(O_2CFc)], two potentials [E_0 = 0.02 V (ΔE_p = 0.136 V), E_0 = 0.18 V (ΔE_p = 0.104 V)] are typical. For **18**, the irreversible reduction for gold(I) was observed at –2.72 V (Figure 8).

Compound **21a** shows, as expected, two reversible processes at E_0 = –0.004 V (ΔE_p = 0.124 V) and E_0 = 0.46 V (ΔE_p = 0.100 V) (Figure 9). The first wave can be ascribed to the oxidation of the ethynylferrocene unit [for comparison, HC≡CFc (E_0 = 0.11 V)].[20] This confirms that the FcC≡C unit in **21a** is easier to oxidize than HC≡CFc. For **21b** also an reversible [Fe^{II}/Fe^{III}] redox couple was observed for the ferrocenyl unit (E_0 = 0.49 V, ΔE_p = 0.142 V), while the ethynylruthenocene moiety is only irreversibly oxidized ($E_{p,ox}$ = 0.35 V), which is typical for ruthenocenyl-containing complexes including HC≡CRc[21] and Ru(η^5-$C_5H_4PPh_2)_2$.[22] The reduction of gold(I) in **21a** appears at $E_{p,red}$ = –2.60 V, while for **21b** this reduction could not be observed.

Conclusions

Hetero(multi)metallic complexes of type [L_nM(O_2C-fcP$Ph_2)_2$] {L_nM = (tmeda)Zn; (pmdta)Zn; [Ti]; fc = ferrocene-1,1′-diyl, (η^5-$C_5H_4)_2Fe$; tmeda = *N*,*N*,*N*′,*N*′-*t*etra*m*ethyl*e*thylene*d*i*a*mine; pmdta = 1,1,4,7,7-*p*enta*m*ethyl*d*iethylene*tri*amine; [Ti] = (η^5-$C_5H_5)_2Ti$}, [$L_nM(X)$(O_2Cfc-PPh_2)] {L_nM = (pmdta)Zn, X = Cl; ML_n = [Ti], X = Me}, R[(O_2CfcPPh_2)AuCl] (R = H, H_2NEt_2), [$L_nM(X)$\{(O_2Cfc-PPh_2)AuCl\}] {L_nM = [Ti], X = Me; L_nM = (pmdta)Zn, X = Cl}, [L_nM\{(O_2CfcPPh_2)AuCl\}$_2$] {ML_n = (tmeda)Zn} and [L_nM\{(O_2CfcPPh_2)AuC≡CR\}$_2$] {L_nM = (tmeda)Zn, R = Fc, Rc; Fc = (η^5-C_5H_5)(η^5-C_5H_4)Fe; Rc = (η^5-C_5H_5)(η^5-C_5H_4)Ru}, featuring two, three, or four different transition-metal atoms including titanium, zinc, iron, gold, and ruthenium, have been synthesized. In these molecules organometallic building blocks are connected with metal–organic units. The synthesis strategy to prepare such molecules is based on consecutive synthesis methodologies by using preformed organometallic and/or metal–organic building blocks. This method enriches the synthesis procedures for the preparation of this new class of heterometallic compounds, and it should be suitable for generalizing to other systems, as well.

The solid-state structures of four compounds, showing typical features for their organometallic and metal–organic

building blocks, were determined. Complex [(H_2NEt_2)-{$(O_2CfcPPh_2)AuCl$}] forms a coordination polymer in the solid state, whereby the stairlike 1D chain is set up by N–H···O hydrogen bonds and intermolecular π–π interactions.

Cyclic voltammetric studies have shown oxidation and reduction processes owing to the corresponding redox centers. For compounds with a noncoordinated PPh_2 group, it is typical that after oxidation of Fe^{II} an intramolecular electron transfer from noncoordinated P^{III} to iron takes place. This results in a species containing Fe^{II} and P^{IV} that is further electrochemically oxidized to give P^{V}. The thus generated ferrocene–phosphane Fe^{II}–P^{V} system then exhibits a reversible [Fe^{II}/Fe^{III}] redox wave. In contrast, this behavior is prevented when the diphenylphosphanyl group is datively bonded to a gold(I) complex fragment. The [Fe^{II}/Fe^{III}] potentials for the $(\eta^5\text{-}C_5H_4)_2Fe$ units are independent of the gold(I)X moieties (X = Cl, C≡CFc, C≡CRc) coordinated by the diphenylphosphanyl group. For [(H_2NEt_2)]{$(O_2Cfc$-$PPh_2)AuCl$}], two waves for the ferrocene/ferrocenium [Fe^{II}/Fe^{III}] redox couple were obtained, most probably because of an equilibrium between the deprotonated and protonated forms of this complex: ([(H_2NEt_2)]{$(O_2CfcPPh_2)AuCl$}]/[$(HO_2CfcPPh_2)AuCl$]).

Experimental Section

Starting Materials, Reaction Conditions, and Instrumentation: All reactions were carried out under an atmosphere of purified nitrogen (4.6) by using standard Schlenk techniques. Tetrahydrofuran, diethyl ether and *n*-hexane were purified by distillation from sodium/benzophenone ketyl; dichloromethane was purified by distillation from calcium hydride. Methanol was purified by distillation from magnesium. Diethylamine and triethylamine were purified by distillation from KOH. Celite (purified and annealed, Erg. B.6, Riedel de Haen) was used for filtrations. Hdpf,[19] [(tmeda)$ZnCl_2$],[23] [(pmdta)$ZnCl_2$],[24] [Ti](Me)$_2$,[25] [Ti]Cl_2,[26] HC≡CFc,[27] HC≡CRc,[28] and [(tht)AuCl][29] were prepared according to published procedures. Infrared spectra were recorded with a Perkin–Elmer FT-IR spectrometer Spectrum 1000. ^{1}H NMR spectra were recorded with a Bruker Avance 250 spectrometer at 298 K operating at 250.130 MHz in the Fourier transform mode; $^{13}C\{^1H\}$ NMR spectra were recorded at 62.860 MHz. Chemical shifts are reported downfield from tetramethylsilane with the solvent as reference signal ($CDCl_3$: ^{1}H NMR δ = 7.26 ppm; $^{13}C\{^1H\}$ NMR δ = 77.16 ppm). $^{31}P\{^1H\}$ NMR spectra were recorded at 101.255 MHz in $CDCl_3$ with $P(OMe)_3$ as external standard (δ = 139.0 ppm) relative to 85% H_3PO_4 (δ = 0.00 ppm). The ESI-TOF (Electro-Spray-Ionization-Time-of-Flight) mass spectra were recorded by using a Mariner Biospectrometry Workstation 4.0 (Applied Biosystems). Cyclic voltammograms were recorded in a dried cell purged with purified argon. Platinum wires served as working and counterelectrodes. A saturated calomel electrode in a separated compartment served as reference electrode. For ease of comparison, all electrode potentials are converted by using the potential of the ferrocene/ferrocenium redox couple FcH/FcH^+ {FcH = $(\eta^5\text{-}C_5H_5)_2$-Fe, E_0 = 0.00 V, ΔE_p = 0.10 V} as reference.[18] Electrolyte solutions were prepared from dichloromethane and $[n\text{Bu}_4\text{N}]PF_6$ (Fluka, dried with an oil vacuum pump). The organometallic complexes were added at c = 0.5 mM. Cyclic voltammograms were recorded with a PGZ 100 instrument (Radiometer). Melting points were determined by using analytically pure samples, sealed off in nitrogen-purged capillaries, with a Gallenkamp MFB 595010M melting point apparatus. Elemental analyses were performed with a Flashea (Thermo Electron Corporation) instrument.

Synthesis and Characterization of [(tmeda)Zn($O_2CfcPPh_2$)$_2$] (3)

Method 1: Hdpf (**1**) (600 mg, 1.449 mmol) was dissolved in methanol (10 mL), and triethylamine (73.2 mg, 0.724 mmol, 0.1 mL) was added in a single portion. After this solution was stirred for 20 min, [(tmeda)$Zn(NO_3)_2$] (**5**) (0.724 mmol) {prepared in situ by treating [(tmeda)$ZnCl_2$] (182.9 mg, 0.724 mmol) (**4**) with [$AgNO_3$] (246 mg, 1.449 mmol) in a mixture of dichloromethane (2 mL) and methanol (6 mL)} was added in a single portion, and the resulting reaction solution was stirred for 1 h at 25 °C. All volatile materials were removed under reduced pressure. The remaining solid material was washed with methanol (2 × 5 mL). After drying with an oil vacuum pump, complex **3** was obtained as a yellow solid. Yield: 503 mg (0.471 mmol, 65% based on **2**).

Method 2: Hdpf (**1**) (100.0 mg, 0.241 mmol) was suspended in methanol (5 mL of) and treated with NaOH (9.7 mg, 0.241 mmol). The resulting reaction solution was stirred for 10 min at 25 °C and then [(tmeda)$ZnCl_2$] (**2**) (30.5 mg, 0.121 mmol) was added in a single portion. Stirring was continued for 2 h at room temperature, and then the solvent was reduced in volume under reduced pressure. The yellow solid obtained was washed with methanol (4 × 2 mL). The residue was then dissolved in dichloromethane (5 mL), dried with Na_2SO_4, and was filtered through a pad of Celite. After removing the solvent with an oil vacuum pump, the title compound was obtained as a yellow solid. Yield: 101 mg (0.100 mmol, 83% based on **2**).

M.p. 122 °C. IR (KBr): $\tilde{\nu}$ = 3055 (w), 3003 (w), 2917 (w), 2847 (w), 1595 (s), 1471 (vs), 1435 (m), 1386 (vs), 1351 (s), 1188 (w), 1158 (w), 1095 (w), 1025 (m), 829 (w), 800 (m), 742 (s), 697 (s), 499 (s), 454 (w) cm^{-1}. ^{1}H NMR (250 MHz, $CDCl_3$, 25 °C): δ = 2.58 (s, 12 H, CH_3), 2.74 (s, 4 H, CH_2), 4.13 (br. s, 8 H, C_5H_4), 4.46 (br. s, 4 H, $C_5H_4PPh_2$), 4.70 (br. s, 4 H, $C_5H_4CO_2$), 5.3 (s, CH_2Cl_2), 7.2–7.4 (m, 20 H, C_6H_5) ppm. $^{13}C\{^1H\}$ NMR (62.82 MHz, $CDCl_3$, 25 °C): δ = 46.92 (*C*H$_3$), 53.5 (*C*H$_2$Cl$_2$), 56.64 (*C*H$_2$), 71.63 (*C*H/*C*$_5$H$_4$CO$_2$), 72.31 (*C*H/*C*$_5$H$_4$CO$_2$), 73.76 (d, J_{PC} = 3 Hz, *C*H/*C*$_5$H$_4$PPh$_2$), 74.05 (d, J_{PC} = 14 Hz, *C*H/*C*$_5$H$_4$PPh$_2$), 75.55 (*C*^{i}/*C*$_5$H$_4$CO$_2$) (please note that the signal of the carbon atom *C*^{i}/C$_5$H$_4$ is covered by the solvent signal), 128.24 (d, $^3J_{PC}$ = 7 Hz, *C*^{m}/*C*$_6$H$_5$), 128.58 (*C*^{p}/*C*$_6$H$_5$), 133.57 (d, $^2J_{PC}$ = 19 Hz, *C*^{o}/*C*$_6$H$_5$), 138.86 (d, $^1J_{PC}$ = 9 Hz, *C*^{i}/*C*$_6$H$_5$), 178.83 (*C*=O) ppm. $^{31}P\{^1H\}$ NMR (101.25 MHz, $CDCl_3$, 25 °C): δ = –18.3 ppm. MS (ESI-TOF): *m*/*z* = 1008 [M$^+$], 893 [M – tmeda +H]$^+$, 595 [M – $O_2CfcPPh_2$]$^+$. $C_{52}H_{52}Fe_2N_2O_4P_2Zn\cdot0.7CH_2Cl_2$ (1067.41): calcd. C 59.30, H 5.04, N 2.62; found C 59.32, H 5.20, N 2.75.

[(pmdta)Zn(Cl)($O_2CfcPPh_2$)] (7): The same synthesis procedure as described for the preparation of **3** (Method 2) was applied for the synthesis of **7**. Starting from Hdpf (**1**) (100.0 mg, 0.241 mmol), NaOH (9.7 mg, 0.241 mmol), and **4** (74.9 mg, 0.241 mmol) gave **7** as a yellow solid. Complex **7** was further purified by crystallization from a dichloromethane solution layered with *n*-hexane at room temperature. Yield: 122 mg (0.177 mmol, 73% based on **4**). M.p. 152 °C. IR (KBr): $\tilde{\nu}$ = 3067 (w), 2972 (w), 2869 (m), 2806 (w), 1581 (s), 1474 (vs), 1435 (m), 1387 (s), 1346 (s), 1305 (w), 1182 (w), 1160 (w), 1106 (w), 1061 (w), 1028 (m), 977 (w), 936 (w), 839 (w), 794 (m), 747 (m), 698 (m), 522 (w), 495 (m) cm^{-1}. ^{1}H NMR (250 MHz, $CDCl_3$, 25 °C): δ = 2.62 (s, 12 H, CH_3), 2.3–3.1 (m, 11 H, CH_3, CH_2), 4.08 (br. s, 2 H, $C_5H_4PPh_2$), 4.11 (br. s, 2 H, $C_5H_4CO_2$), 4.49 (br. s, 2 H, $C_5H_4PPh_2$), 4.62 (br. s, 2 H, $C_5H_4CO_2$), 5.3 (s, CH_2Cl_2), 7.2–7.4 (m, 10 H, C_6H_5) ppm. $^{13}C\{^1H\}$ NMR (62.82 MHz, $CDCl_3$, 25 °C): δ = 43.35 (*C*H$_3$), 46.85 (*C*H$_3$), 53.5 (*C*H$_2$Cl$_2$), 55.47 (*C*H$_2$),

56.75 (CH_2), 71.33 ($CH/C_5H_4CO_2$), 71.66 ($CH/C_5H_4CO_2$), 73.62 (d, J_{PC} = 3 Hz, $CH/C_5H_4PPh_2$), 73.85 (d, J_{PC} = 15 Hz, $CH/C_5H_4PPh_2$), 76.26 (d, J_{PC} = 6 Hz, $C^i/C_5H_4PPh_2$) (please note that the signal of the carbon atom C^i/C_5H_4 is covered by the solvent signal), 128.20 (d, $^3J_{PC}$ = 7 Hz, C^m/C_6H_5), 128.50 (C^p/C_6H_5), 133.60 (d, $^2J_{PC}$ = 19 Hz, C^o/C_6H_5), 139.21 (d, $^1J_{PC}$ = 10 Hz, C^i/C_6H_5), 175.90 (C=O) ppm. $^{31}P\{^1H\}$ NMR (101.25 MHz, $CDCl_3$, 25 °C): δ = –18.1 ppm. MS (ESI-TOF): m/z = 650 $[M - Cl - H]^+$. $C_{32}H_{41}ClFeN_3O_2PZn{\cdot}0.1CH_2Cl_2$ (693.52): calcd. C 55.54, H 5.99, N 6.11; found C 55.42, H 5.88, N 5.81.

[(pmdta)Zn(O_2CfcPPh$_2$)$_2$] (8): Hdpf (**1**) (100.0 mg, 0.241 mmol) was reacted under the same conditions as described for the preparation of **3** (Method 2) with [(pmdta)$ZnCl_2$] (**2**) (37.4 mg, 0.121 mmol). After appropriate work-up, complex **8** was obtained as a yellow solid. Yield: 110 mg (0.103 mmol, 85% based on **4**). M.p. 97 °C. IR (KBr): $\tilde{\nu}$ = 3428 (br. m), 3050 (m), 3268 (m), 3265 (m), 2799 (m), 2215 (w), 2014 (w), 1962 (w) 1766 (m), 1592 (vs), 1467 (vs), 1434 (m), 1383 (vs), 1339 (vs), 1304 (m), 1250 (m), 1184 (m), 1158 (m), 1100 (m), 1059 (m), 1026 (s), 933 (m), 911 (m), 800 (s), 743 (s), 697 (s), 636 (w), 569 (w), 495 (s), 452 (m) cm^{-1}. ^1H NMR (250 MHz, $CDCl_3$, 25 °C): δ = 2.45 (s, 3 H, CH_3), 2.61 (s, 12 H, CH_3), 2.3–3.1 (m, 8 H, CH_2), 4.06 (br. s, 4 H, $C_5H_4PPh_2$), 4.09 (br. s, 4 H, $C_5H_4CO_2$), 4.42 (br. s, 4 H, $C_5H_4PPh_2$), 4.63 (br. s, 4 H, $C_5H_4CO_2$), 7.2–7.4 (m, 20 H, C_6H_5) ppm. $^{13}C\{^1H\}$ NMR (62.82 MHz, $CDCl_3$, 25 °C): δ = 43.25 (CH_3), 46.92 (CH_3), 55.35 (CH_2), 56.86 (CH_2), 71.26 ($CH/C_5H_4CO_2$), 71.29 ($CH/C_5H_4CO_2$), 73.21 (br. s, $CH/C_5H_4PPh_2$), 73.60 (d, J = 15 Hz, $CH/C_5H_4PPh_2$), 76.05 (d, J = 7 Hz, $C^i/C_5H_4PPh_2$), 79.10 (br. s, $C^i/C_5H_4CO_2$), 128.12 (d, $^3J_{PC}$ = 7 Hz, C^m/C_6H_5), 128.40 (C^p/C_6H_5), 133.51 (d, $^2J_{PC}$ = 19 Hz, C^o/C_6H_5), 139.20 (d, $^1J_{PC}$ = 10 Hz, C^i/C_6H_5), 175.45 (C=O) ppm. $^{31}P\{^1H\}$ NMR (101.25 MHz, $CDCl_3$, 25 °C): δ = –18.3 ppm. MS (ESI-TOF): m/z = 652 $[M - O_2CfcPPh_2]^+$. $C_{55}H_{59}Fe_2N_3O_4P_2Zn$ (1065.06): calcd. C 62.07, H 5.59, N 3.95; found C 62.18, H 5.66, N 3.85.

[Ti](Me)(O_2CfcPPh$_2$) (10): Hdpf (**1**) (100 mg, 0.241 mmol) was dissolved in tetrahydrofuran (8 mL) and [Ti]Me_2 (**9**) (50.3 mg, 0.241 mmol), dissolved in tetrahydrofuran (2 mL), was slowly added. After this reaction solution was stirred for 25 min at room temperature, all volatiles were removed under reduced pressure, and the residue was washed with *n*-hexane (2 × 3 mL) and dried with an oil vacuum pump to give **10** as an orange solid. Yield: 140 mg (0.231 mmol, 96% based on Hdpf). M.p. 63 °C. IR (KBr): $\tilde{\nu}$ = 1702 (w), 1630 (vs), 1452 (s), 1377 (s), 1302 (vs), 1170 (s), 1120 (w), 1100 (m), 1077 (w), 1053 (w), 1025 (s), 919 (w), 823 (vs), 782 (m), 745 (m), 695 (s), 667 (w), 643 (w), 621 (w), 574 (m), 530 (w), 489 (m), 464 (w), 444 (w) cm^{-1}. ^1H NMR (250 MHz, $CDCl_3$, 25 °C): δ = 0.95 (s, 3 H, CH_3), 4.12 (dpt, J_{PH} = 1.8, J_{HH} = 1.8 Hz, 2 H, $C_5H_4PPh_2$), 4.15 (pt, J_{HH} = 2.0 Hz, 2 H, $C_5H_4CO_2$), 4.39 (pt, J_{HH} = 2.0 Hz, 2 H, $C_5H_4PPh_2$), 4.41 (pt, J_{HH} = 1.8 Hz, 2 H, $C_5H_4CO_2$), 5.3 (s, CH_2Cl_2), 6.18 (s, 10 H, C_5H_5), 7.2–7.4 (m, 10 H, C_6H_5) ppm. $^{13}C\{^1H\}$NMR (62.82 MHz, $CDCl_3$, 25 °C): δ = 44.12 (CH_3), 53.5 (CH_2Cl_2), 71.15 ($CH/C_5H_4CO_2$), 72.18 ($CH/C_5H_4CO_2$), 72.85 (d, J_{CP} = 3 Hz, $CH/C_5H_4PPh_2$), 73.77 (d, J_{CP} = 14 Hz, $CH/C_5H_4PPh_2$), 76.10 ($C^i/C_5H_4CO_2$), 77.40 (d, J_{CP} = 8 Hz, $C^i/C_5H_4PPh_2$), 114.73 (C_5H_5), 128.32 (d, $^3J_{PC}$ = 7 Hz, C^m/C_6H_5), 128.69 (C^p/C_6H_5), 133.58 (d, $^2J_{PC}$ = 19 Hz, C^o/C_6H_5), 138.83 (d, $^1J_{PC}$ = 10 Hz, C^i/C_6H_5), 175.40 (C=O) ppm. $^{31}P\{^1H\}$NMR (101.25 MHz, $CDCl_3$, 25 °C): δ = –18.9 ppm. MS (ESI-MS): m/z = 607 $[M + H]^+$. $C_{34}H_{31}FeO_2PTi{\cdot}0.1CH_2Cl_2$ (614.48): calcd. C 66.59, H 5.12; found C 66.70, H 5.16.

[Ti](O_2CfcPPh$_2$)$_2$ (12): Triethylamine (0.03 mL, 0.248 mmol) was added to Hdpf (**1**) (100 mg, 0.241 mmol) dissolved in tetrahydrofuran (10 mL). To this solution, [Ti]Cl_2 (**11**) (25.1 mg, 0.121 mmol) was added in a single portion. After being stirred for 4.5 h at 25 °C, the reaction mixture was filtered through a pad of Celite, and the solvent was reduced in volume (3 mL). On addition of diethyl ether (10 mL), an orange solid precipitated, which was washed with methanol (3 × 4 mL). After it was dried with an oil vacuum pump, molecule **12** was obtained as a pale orange solid. Yield: 68 mg (0.068 mmol, 56% based on [Ti]Cl_2). M.p. 170 °C (dec.). IR (KBr): $\tilde{\nu}$ = 1637 (vs), 1477 (w), 1457 (m), 1434 (w), 1372 (m), 1318 (m), 1285 (s), 1261 (m), 1168 (s), 1093 (m), 1027 (m), 829 (s), 806 (m), 743 (m), 697 (m), 658 (w), 500 (m) cm^{-1}. ^1H NMR (250 MHz, $CDCl_3$, 25 °C): δ = 1.1 (s, CH_3OH), 3.5 (s, CH_3OH), 4.17 (dpt, J_{PH} = 1.8, J_{HH} = 1.8 Hz, 4 H, $C_5H_4PPh_2$), 4.22 (pt, J_{HH} = 1.9 Hz, 4 H, $C_5H_4CO_2$), 4.38 (pt, J_{HH} = 1.8 Hz, 4 H, $C_5H_4PPh_2$), 4.41 (pt, J_{HH} = 1.9 Hz, 4 H, $C_5H_4CO_2$), 6.58 (s, 10 H, C_5H_5), 7.2–7.4 (m, 20 H, C_6H_5) ppm. $^{13}C\{^1H\}$NMR (62.82 MHz, $CDCl_3$, 25 °C): δ = 50.4 (CH_3OH), 71.53 ($CH/C_5H_4CO_2$), 72.25 ($CH/C_5H_4CO_2$), 72.65 (d, J_{CP} = 3 Hz, $CH/C_5H_4PPh_2$), 73.93 (d, J_{CP} = 14 Hz, $CH/C_5H_4PPh_2$), 76.43 ($C^i/C_5H_4CO_2$) (please note that the signal of the carbon atom C^i/C_5H_4 is covered by the solvent signal), 118.30 (C_5H_5), 128.37 (d, $^3J_{PC}$ = 7 Hz, C^m/C_6H_5), 128.75 (C^p/C_6H_5), 133.63 (d, $^2J_{PC}$ = 20 Hz, C^o/C_6H_5), 138.77 (d, $^1J_{PC}$ = 10 Hz, C^i/C_6H_5), 176.19 (C=O) ppm. $^{31}P\{^1H\}$NMR (101.25 MHz, $CDCl_3$, 25 °C): δ = –19.1 ppm. $C_{56}H_{46}Fe_2O_4P_2Ti{\cdot}0.5CH_3OH$ (1020.12): calcd. C 66.46, H 4.74; found C 66.45, H 5.28.

[(Hdpf)AuCl] (14): Hdpf (**1**) (100.0 mg, 0.241 mmol) was dissolved in tetrahydrofuran (8 mL) and slowly added to [(tht)AuCl] (**13**) (77.4 mg, 0.241 mmol) dissolved in tetrahydrofuran (8 mL) at 0 °C. The resulting reaction solution was stirred for 15 min at 0 °C and then for 5 min at 25 °C. The solvent was reduced in volume, and the product was precipitated by addition of *n*-hexane (10 mL). This procedure was repeated three times. Removal of all volatiles with an oil vacuum pump gave **14** as a yellow-orange solid. Yield: 145 mg (0.224 mmol, 93% based on **1**). M.p. 114 °C (dec.). IR (KBr): $\tilde{\nu}$ = 1673 (vs), 1476 (s), 1434 (m), 1400 (w), 1366 (w), 1291 (s), 1166 (m), 1102 (m), 1069 (w), 1030 (m), 998 (w), 940 (w), 911 (w), 837 (m), 754 (m), 743 (m), 700 (m), 657 (m), 526 (m), 506 (m), 496 (m), 478 (m), 455 (w) cm^{-1}. ^1H NMR (250 MHz, $CDCl_3$, 25 °C): δ = 1.85 (m, thf), 3.75 (m, thf), 4.45 (dpt, J_{PH} = 2.8, J_{HH} = 1.9 Hz, 2 H, $C_5H_4PPh_2$), 4.54 (pt, J_{HH} = 2.0 Hz, 2 H, $C_5H_4CO_2$), 4.65 (br. s, 2 H, $C_5H_4PPh_2$), 4.82 (pt, J_{HH} = 2.0 Hz, 2 H, $C_5H_4CO_2$), 7.4–7.6 (m, 20 H, C_6H_5) ppm. $^{13}C\{^1H\}$ NMR (62.82 MHz, $CDCl_3$, 25 °C): δ = 12.6 (thf), 68.0 (thf), 72.39 ($CH/C_5H_4CO_2$), 74.54 ($CH/C_5H_4CO_2$), 74.97 (d, J_{PC} = 8 Hz, $CH/C_5H_4PPh_2$), 75.15 (d, J_{PC} = 3 Hz, $CH/C_5H_4PPh_2$) (please note that the signal of the carbon atom C^i/C_5H_4 is covered by the solvent signal), 129.18 (d, $^3J_{PC}$ = 12 Hz, C^m/C_6H_5), 130.27 (d, $^1J_{PC}$ = 64 Hz, C^i/C_6H_5), 132.04 (d, $^4J_{PC}$ = 3 Hz, C^p/C_6H_5), 133.67 (d, $^2J_{PC}$ = 14 Hz, C^o/C_6H_5), 167.07 (C=O) ppm. $^{31}P\{^1H\}$ NMR (101.25 MHz, $CDCl_3$, 25 °C): δ = 26.6 ppm. $C_{23}H_{19}AuClFeO_2P{\cdot}0.4thf$ (674.81): calcd. C 43.74, H 3.32; found C 43.78, H 3.23.

[Ti](Me){(O_2CfcPPh$_2$)AuCl}] (15): Compound **10** (59 mg, 0.098 mmol) dissolved in tetrahydrofuran (4 mL) was slowly added to **13** (31 mg, 0.098 mmol) in tetrahydrofuran (5 mL) at 0 °C. The decomposition was visible after two minutes of stirring at 0 °C. Running the reaction at –60 °C also resulted in decomposition, albeit after 10 min of stirring. $C_{34}H_{31}AuClFeO_2PTi$ (838.71). MS (ESI-TOF): m/z = 803 $[M - Cl]^+$, 891 $[M + CH_3OH + Na - 2H]^+$. Further characterization was not possible, because **15** was very unstable in solution.

[(pmdta)Zn(Cl){(O_2CfcPPh$_2$)AuCl}] (16): Complex **8** (50 mg, 0.073 mmol) was dissolved in tetrahydrofuran (3 mL) and was

slowly added to **13** (23 mg, 0.073 mmol) dissolved in tetrahydrofuran (5 mL) at 0 °C. After this mixture was stirred for 15 min at this temperature and worked up as described for the synthesis of **14**, the title complex could be isolated as a pale yellow solid. Yield: 63 mg (0.070 mmol, 96% based on **8**). M.p. 118 °C (dec.). IR (KBr): $\tilde{\nu}$ = 2978 (w), 2921 (w), 2890 (w), 1585 (s), 1471 (vs), 1439 (m), 1387 (s), 1348 (s), 1307 (w), 1258 (w), 1177 (m), 1103 (m), 1058 (w), 1028 (m), 939 (w), 800 (m), 751 (m), 697 (m), 628 (w), 556 (m), 502 (m) cm^{-1}. ^{1}H NMR (250 MHz, $CDCl_3$, 25 °C): δ = 2.64 (s, 12 H, CH_3), 2.3–3.1 (m, 11 H, CH_3, CH_2), 4.29 (br. s, 2 H, C_5H_4), 4.39 (br. s, 2 H, C_5H_4), 4.67 (br. s, 2 H, C_5H_4), 4.77 (br., 2 H, C_5H_4), 7.3–7.7 (m, 10 H, C_6H_5) ppm. ^{31}P{^{1}H} NMR (101.25 MHz, $CDCl_3$, 25 °C): δ = 27.4 ppm. $C_{32}H_{41}AuCl_2FeN_3O_2PZn$ (917.06): calcd. C 41.81, H 4.51, N 4.58; found C 41.32, H 4.31, N 4.07.

[(tmeda)Zn{(O_2CfcPPh$_2$)AuCl}$_2$] (17): The same synthesis procedure as described for the preparation of **14** was applied for the synthesis of **17**, starting from **3** (30 mg, 0.030 mmol) in tetrahydrofuran (2 mL) and **13** (19.1 mg, 0.060 mmol) in tetrahydrofuran (2 mL). After appropriate work-up, the title complex could be isolated as a pale yellow solid. Yield: 40 mg (0.027 mmol, 90% based on **3**). M.p. 175 °C (dec.). IR (KBr): $\tilde{\nu}$ = 3101 (w), 2964 (w), 2924 (w), 2848 (w), 1600 (s), 1475 (vs), 1437 (m), 1388 (vs), 1355 (s), 1174 (m), 1103 (m), 1030 (m), 836 (w), 801 (w), 750 (m), 562 (w), 506 (w) cm^{-1}. ^{1}H NMR (250 MHz, $CDCl_3$, 25 °C): δ = 2.55 (s, 12 H, CH_3), 2.75 (s, 4 H, CH_2), 4.30 (br. s, 4 H, C_5H_4), 4.33 (br. s, 4 H, C_5H_4), 4.63 (br. s, 4 H, C_5H_4), 4.76 (br. s, 4 H, C_5H_4), 7.3–7.6 (m, 20 H, C_6H_5) ppm. ^{13}C{^{1}H} NMR (62.82 MHz, $CDCl_3$, 25 °C): δ = 47.04 (*C*H$_3$), 56.63 (*C*H$_2$), 72.39 (*C*H/$C_5H_4CO_2$), 73.54 (*C*H/$C_5H_4CO_2$), 74.50 (d, J_{PC} = 14 Hz, *C*H/$C_5H_4PPh_2$), 75.67 (d, J_{PC} = 8 Hz, *C*H/$C_5H_4PPh_2$) (please note that the signal of the carbon atom C^i/C_5H_4 is covered by the solvent signal), 129.03 (d, $^3J_{PC}$ = 12 Hz, C^m/C_6H_5), 130.58 (d, $^1J_{PC}$ = 64 Hz, C^i/C_6H_5), 131.82 (C^p/C_6H_5), 133.58 (d, $^2J_{PC}$ = 14 Hz, C^o/C_6H_5) ppm (please note that the CO resonance signal could not be detected under the measurement conditions used). ^{31}P{^{1}H} NMR (101.25 MHz, $CDCl_3$, 25 °C): δ = 27.1 ppm. MS (ESI-TOF): *m*/*z* = 1437 [M – Cl]$^+$. $C_{52}H_{52}Au_2Cl_2Fe_2N_2O_4P_2Zn$ (1470.01): calcd. C 42.45, H 3.57, N 1.91; found C 42.47, H 3.07, N 1.30.

[(H_2NEt$_2$){(O_2CfcPPh$_2$)AuCl}] (18): Diethylamine (5 mL) was added to **14** (80.0 mg, 0.124 mmol) dissolved in tetrahydrofuran (1 mL). This reaction solution was stirred for 1 h at 25 °C. The solvent was removed under reduced pressure, and the residue was washed with diethylamine (2 × 2 mL), whereby the title compound was obtained as a yellow solid. Yield: 85 mg (0.118 mmol, 95% based on **14**). M.p. 132 °C (dec.). IR (KBr): $\tilde{\nu}$ = 3048 (w), 2982 (w), 2925 (w), 2853 (w), 2488 (w), 1624 (s), 1561 (m), 1545 (m), 1463 (vs), 1436 (s), 1385 (vs), 1348 (s), 1261 (m), 1174 (m), 1102 (s), 1070 (m), 1026 (s), 806 (s), 781 (m), 747 (m), 695 (s), 554 (m), 528 (m), 501 (m), 478 (m) cm^{-1}. ^{1}H NMR (250 MHz, $CDCl_3$, 25 °C): δ = 1.33 (t, 6 H, CH_3), 2.97 (q, 4 H, CH_2), 4.24 (br. s, 2 H, C_5H_4), 4.37 (br. s, 2 H, C_5H_4), 4.58 (br. s, 2 H, C_5H_4), 4.82 (br. s, 2 H, C_5H_4), 7.4–7.8 (m, 10 H, C_6H_5) ppm. ^{13}C{^{1}H} NMR (62.82 MHz, $CDCl_3$, 25 °C): δ = 12.06 (*C*H$_3$), 42.23 (*C*H$_2$), 71.85 (*C*H/$C_5H_4CO_2$), 72.89 (*C*H/$C_5H_4CO_2$), 74.23 (d, J_{PC} = 14 Hz, *C*H/$C_5H_4PPh_2$), 75.00 (d, J_{PC} = 8 Hz, *C*H/$C_5H_4PPh_2$), 80.23 (*C*H/$C_5H_4CO_2$) (please note that the signal of the carbon atom C^i/C_5H_4 is covered by the solvent signal), 129.04 (d, $^3J_{PC}$ = 12 Hz, C^m/C_6H_5), 130.90 (d, $^1J_{PC}$ = 64 Hz, C^i/C_6H_5), 131.78 (C^p/C_6H_5), 133.70 (d, $^2J_{PC}$ = 15 Hz, C^o/C_6H_5), 175.07 (*C*=O) ppm. ^{31}P{^{1}H} NMR (101.25 MHz, $CDCl_3$, 25 °C): δ = 27.0 ppm. $C_{27}H_{30}AuClFeNO_2P$ (719.07): calcd. C 45.06, H 4.20, N 1.95; found C 45.12, H 4.24, N 1.55.

[(tmeda)Zn{(O_2CfcPPh$_2$)AuC≡CFc}$_2$] (21a): Compound **14** (80 mg, 0.124 mmol) was suspended in diethylamine (8 mL), and HC≡CFc (**19a**) (28.6 mg, 0.136 mmol) was added in a single portion. After this mixture was stirred for 24 h at 25 °C, the solvent was reduced in volume to 3 mL, followed by addition of *n*-hexane (10 mL). The precipitate was washed with *n*-hexane (2 × 5 mL). The obtained residue was dissolved in methanol (8 mL), and **2** (15.7 mg, 0.062 mmol) was added in a single portion. Immediately, an orange precipitate formed. Stirring was continued for 45 min. The supernatant solution was decanted, and the remaining solid was washed with methanol (4 × 2 mL) followed by dissolving in dichloromethane and precipitation with *n*-hexane. Removal of all volatiles with an oil vacuum pump afforded **21a** as a pale orange material. Yield: 80 mg (0.044 mmol, 71% based on **2**). M.p. 104 °C (dec.). IR (KBr): $\tilde{\nu}$ = 3084 (m), 2960 (m), 2922 (m), 2847 (w), 2107 (m) ($\nu_{C\equiv C}$), 1591 (vs), 1477 (vs), 1434 (m), 1389 (s), 1353 (s), 1310 (w), 1258 (m), 1175 (m), 1102 (s), 1028 (s), 920 (w), 804 (s), 748 (m), 695 (s), 549 (m), 525 (s) 501 (s) cm^{-1}. ^{1}H NMR (250 MHz, $CDCl_3$, 25 °C): δ = 2.58 (s, 12 H, CH_3), 2.72 (s, 4 H, CH_2), 4.13 (br. s, 4 H, C_5H_4), 4.23 (s, 10 H, C_5H_5), 4.36 (br. s, 4 H, C_5H_4), 4.43 (br. s, 4 H, C_5H_4), 4.46 (br. s, 4 H, C_5H_4), 4.66 (br. s, 4 H, C_5H_4), 4.73 (br. s, 4 H, C_5H_4), 5.3 (s, CH_2Cl_2), 7.3–7.7 (m, 20 H, C_6H_5) ppm. ^{13}C{^{1}H} NMR (62.82 MHz, $CDCl_3$, 25 °C): δ = 46.81 (*C*H$_3$), 53.5 (*C*H$_2$Cl$_2$), 56.69 (*C*H$_2$), 67.95 (*C*H/C_5H_4), 70.15 (C_5H_5), 71.99 (*C*H/C_5H_4), 72.22 (*C*H/$C_5H_4CO_2$), 73.21 (*C*H/$C_5H_4CO_2$), 74.66 (d, J_{PC} = 13 Hz, *C*H/$C_5H_4PPh_2$), 75.62 (d, J_{PC} = 6 Hz, *C*H/$C_5H_4PPh_2$), 128.92 (d, $^3J_{PC}$ = 12 Hz, C^m/C_6H_5), 131.34 (m, C^i and C^p/C_6H_5), 133.89 (d, $^2J_{PC}$ = 14 Hz, C^o/C_6H_5) ppm (please note that the carbon signals of *C*O and C^i/C_5H_4 could not be detected under the measurement conditions applied). ^{31}P{^{1}H} NMR (101.25 MHz, $CDCl_3$, 25 °C): δ = 36.1 ppm. MS (ESI-MS): *m*/*z* = 1609 [M – C_2Fc]$^+$, 1203 [M – C_2Fc – AuC_2Fc]$^+$. $C_{76}H_{70}Au_2Fe_4N_2O_4P_2Zn1{\cdot}2CH_2Cl_2$ (1918.83): calcd. C 48.28, H 3.80, N 1.46; found C 48.27, H 3.68, N 1.50.

[(tmeda)Zn{(O_2CfcPPh$_2$)AuC≡CRc}$_2$] (21b): The same conditions as those used in the synthesis of **21a** were applied to prepare **21b**. The reactants used were **14** (80 mg, 0.124 mmol), HC≡CRc (**19b**) (34.7 mg, 0.136 mmol), and **2** (15.7 mg, 0.062 mmol). After appropriate work-up, the title complex could be isolated as a pale yellow solid. Yield: 51 mg (0.027 mmol, 68% based on **2**). M.p. 109 °C (dec.). IR (KBr): $\tilde{\nu}$ = 433 (m), 2961 (w), 2918 (w), 2104 (w) ($\nu_{C\equiv C}$), 1587 (vs), 1476 (vs), 1436 (s), 1388 (s), 1350 (s), 1172 (m), 1101 (s), 1028 (s). 998 (w), 952 (w), 917 (m), 806 (s), 748 (s), 696 (s), 666 (w), 627 (w), 550 (m), 508 (s), 436 (m) cm^{-1}. ^{1}H NMR (250 MHz, $CDCl_3$, 25 °C): δ = 2.58 (s, 12 H, CH_3), 2.74 (s, 4 H, CH_2), 4.31 (br. s, 4 H, C_5H_4), 4.41 (br. s, 4 H, C_5H_4), 4.49 (br. s, 4 H, C_5H_4), 4.60 (s, 10 H, C_5H_5), 4.66 (br. s, 4 H, C_5H_4), 4.71 (br. s, 4 H, C_5H_4), 4.88 (br. s, 4 H, C_5H_4), 7.3–7.6 (m, 20 H, C_6H_5) ppm. ^{13}C{^{1}H} NMR (62.82 MHz, $CDCl_3$, 25 °C): δ = 46.76 (*C*H$_3$), 56.69 (*C*H$_2$), 69.95 (*C*H/C_5H_4), 71.90 (C_5H_5), 72.3 (*C*H/C_5H_4), 73.12 (*C*H/$C_5H_4CO_2$), 74.46 (*C*H/$C_5H_4CO_2$), 74.85 (d, J_{PC} = 14 Hz, *C*H/$C_5H_4PPh_2$), 75.68 (d, J_{PC} = 11 Hz, *C*H/$C_5H_4PPh_2$), 128.90 (d, $^3J_{PC}$ = 11 Hz, C^m/C_6H_5), 131.30 (m, C^i and C^p/C_6H_5), 133.85 (d, $^2J_{PC}$ = 13 Hz, C^o/C_6H_5) ppm, (the signals of *C*O and C^i/C_5H_4 could not be detected under the measurement conditions applied). ^{31}P{^{1}H} NMR (101.25 MHz, $CDCl_3$, 25 °C): δ = 36.0 ppm. MS (ESI-MS): *m*/*z* = 1655 [M – C_2Rc]$^+$, 1203 [M – C_2Rc – AuC_2Rc]$^+$. $C_{76}H_{70}Au_2Fe_2N_2O_4P_2Ru_2Zn$ (1910.48): calcd. C 47.78, H 3.69, N 1.47; found C 47.65, H 3.65, N 0.95.

Crystal Structure Determination

Crystal data for **3**, **8**, **12**, and **18** are summarized in Table 5. All data were collected on an Oxford Gemini S diffractometer at 293 K

Table 5. Crystallographic data and structure refinement parameters for **3**, **7**, **12**, and **18**.

	3	**7**	**12**	**18**
Formula weight	1007.97	2214.82	1004.47	719.07
Empirical formula	$C_{52}H_{52}Fe_2N_2O_4P_2Zn$	$C_{97.80}H_{126.60}Cl_{16.60}Fe_3N_9O_6P_3Zn_3$	$C_{56}H_{46}Fe_2O_4P_2Ti$	$C_{27}H_{30}AuClFeNO_2P$
Crystal system	monoclinic	triclinic	monoclinic	monoclinic
Space group	*P*2/*c*	$P\bar{1}$	*C*2/*c*	$P2_1/n$
a [Å]	9.5340(10)	8.05630(10)	37.2598(13)	21.2457(4)
b [Å]	7.3481(5)	28.0404(2)	7.4541(3)	11.3505(2)
c [Å]	35.514(4)	28.0429(4)	32.4510(15)	33.7217(6)
α [°]	90	119.0970(10)	90	90
β [°]	92.276(8)	95.4620(10)	95.305(4)	104.021(2)
γ [°]	90	95.4830(10)	90	90
V [Å^3]	2486.0(4)	5436.57(11)	8974.3(6)	7889.7(2)
$\rho_{calcd.}$ [g cm^{-3}]	1.347	1.353	1.487	1.818
F(000)	1044	2299	4144	4224
Crystal size dimensions	0.4 × 0.3 × 0.1	0.4 × 0.2 × 0.2	0.05 × 0.05 × 0.03	0.1 × 0.08 × 0.03
Z	2	2	8	12
Max. and min. transmission	1.01902, 0.97971	1.00000, 0.50772	1.00000, 0.92226	1.00000, 0.50078
μ [mm^{-1}]	1.163	6.179	0.933	6.311
θ [°]	3.07–26.10	3.17–60.37	2.79–26.04	2.85–26.08
Total reflections	19057	40999	28428	47684
Unique reflections	4850	15881	8719	15409
R_{int}	0.0310	0.0292	0.1353	0.0509
Data/restraints/parameters	4885/130/331	15881/0/1189	8719/0/586	15409/174/943
R_1,[a] wR_2[a] [$I \geq 2\sigma(I)$]	0.0485, 0.1413	0.0447, 0.1262	0.0475, 0.0491	0.0890, 0.1881
R_1,[a] wR_2[a] (all data)	0.0832, 0.1547	0.0552, 0.1348	0.1770, 0.0693	0.1099, 0.1954
$\Delta\rho$ [e Å^{-3}]	1.480, –0.263	1.378, –0.510	0.666, –0.467	7.596, –2.724[b]

[a] $R_1 = \Sigma(||F_o| - |F_c||)/\Sigma(|F_o|)$; $wR_2 = \{\Sigma[w(F_o^2 - F_c^2)^2]/\Sigma(wF_o^4)\}^{1/2}$. $S = [\Sigma w(F_o^2 - F_c^2)^2]/(n - p)^{1/2}$. n = number of reflections, p = parameters used. [b] The highest unrefined electron density (Q peaks) for **18** is located at a distance below 0.95 Å around Au: {*d*[Au(1)–Q(1)] = 0.945 Å; 7.6 e Å^{-3}; *d*[Au(3)–Q(3)] = 0.934 Å; 4.02 e Å^{-3}}. According to refs.,[33,34] this might be observed for heavy atoms, for which remaining electron density peaks with ca. 10% of the electron density of the heavy atom are expected to be observed at a distance between 0.60 and 1.20 Å.

(**3**) or 100 K (**8**, **12**, **18**) using Mo-K_α radiation (λ = 0.71 Å) (**3**, **12**, **18**) or Cu-K_α radiation (λ = 1.54 Å) (**8**). For protection against oxygen and moisture, the preparation of the single crystals was performed in perfluoro alkyl ether (ABCR GmbH&Co KG; viscosity 1600 cSt). The structures were solved by direct methods using SHELXS-97[30] (**3**, **8**) or SIR-92[31] (**12**, **18**) and refined by full-matrix least-square procedures on F^2 using SHELXL-97.[32] All non-hydrogen atoms were refined anisotropically, and a riding model was employed in the refinement of the hydrogen atom positions. In **3**, atoms C18 to C23 are disordered and have been refined to split occupancies of 0.47/0.53.

CCDC-682002 (for **3**), -682003 (for **7**), -682005 (for **12**), and -682004 (for **18**) contain the supplementary crystallographic data for this paper. These data can be obtained free of charge from the Cambridge Crystallographic Data Centre via www.ccdc.cam.ac.uk/data_request/cif.

Acknowledgments

We are grateful to the Deutsche Forschungsgemeinschaft and the Fonds der Chemischen Industrie for generous financial support.

[1] For example see: a) J. Kühnert, M. Lamač, T. Rüffer, B. Walfort, P. Štěpnička, H. Lang, *J. Organomet. Chem.* **2007**, *692*, 4303; b) R. Packheiser, H. Lang, *Eur. J. Inorg. Chem.* **2007**, 3786; c) H. Lang, R. Packheiser, B. Walfort, *Organometallics* **2006**, *25*, 1836; d) H. Lang, R. Packheiser, *Collect. Czech. Chem. Commun.* **2007**, *72*, 435; e) M. I. Bruce, P. A. Humphrey, M. Jevric, G. J. Perkins, B. W. Skelton, A. H. White, *J. Organomet. Chem.* **2007**, *692*, 1748; f) N. J. Long, C. K. Williams, *Angew. Chem. Int. Ed.* **2003**, *42*, 2586; g) P. J. Low, R. L. Roberts, R. L. Cordiner, F. Hartl, *J. Solid State Electrochem.* **2005**, *9*, 717; h) V. W.-W. Yam, *J. Organomet. Chem.* **2004**, *689*, 1393; i) M. Samoc, N. Gauthier, M. P. Cifuentes, F. Paul, C. Lapinte, M. G. Humphrey, *Angew. Chem. Int. Ed.* **2006**, *45*, 7376; j) J. Vicente, M.-T. Chicote, M. M. Alvarez-Flacón, *Organometallics* **2005**, *24*, 2764; k) S. H.-F. Chong, S. C.-F. Lam, V. W.-W. Yam, N. Zhu, K.-K. Cheung, *Organometallics* **2004**, *23*, 4924; l) G. Vives, A. Carella, J.-P. Launay, G. Rapenne, *Chem. Commun.* **2006**, 2283; m) S. Szafert, J. A. Gladysz, *Chem. Rev.* **2003**, *103*, 4175; n) M. I. Bruce, K. Costuas, T. Davin, B. G. Ellis, J.-F. Halet, C. Lapinte, P. J. Low, M. E. Smith, B. W. Skelton, L. Toupet, A. H. White, *Organometallics* **2005**, *24*, 3864; o) C. E. Powell, M. G. Humphrey, *Coord. Chem. Rev.* **2004**, *248*, 725; p) F. Paul, C. Lapinte, *Coord. Chem. Rev.* **1998**, *178–180*, 431.

[2] a) H. Jiao, K. Costuas, J. A. Gladysz, J.-F. Halet, M. Guillemot, L. Toupet, F. Paul, C. Lapinte, *J. Am. Chem. Soc.* **2003**, *125*, 9511; b) A. Mayboroda, P. Comba, H. Pritzkow, G. Rheinwald, H. Lang, G. van Koten, *Eur. J. Inorg. Chem.* **2003**, 1703; c) W. Skibar, H. Kopacka, K. Wurst, C. Salzmann, K.-H. Ongania, F. Fabrizi de Biani, P. Zanello, B. Bildstein, *Organometallics* **2004**, *23*, 1024; d) A. Ceccon, S. Santi, L. Orian, A. Bisello, *Coord. Chem. Rev.* **2004**, *248*, 683; e) T. Döhler, H. Görls, D. Walther, *Chem. Commun.* **2000**, 945.

[3] For example see: a) T. Baumgartner, M. Fiege, F. Pontzen, R. Arteaga-Mueller, *Organometallics* **2006**, *25*, 5657; b) J. Kühnert, M. Dušek, J. Demel, H. Lang, P. Štěpnička, *Dalton Trans.* **2007**, 2802; c) L. E. Hagopian, A. N. Campbell, J. A. Golen, A. L. Rheingold, C. Nataro, *J. Organomet. Chem.* **2006**, *691*, 4890; d) F. Zapata, A. Caballero, A. Espinosa, A. Tárraga, P. Molina, *Org. Lett.* **2007**, *9*, 2385; e) J. Ludvíc, P. Štěpnička, *ECS Trans.* **2007**, *2*, 17; f) P. Debroy, S. Roy, *Coord. Chem. Rev.* **2007**, *251*, 203; g) T.-Y. Dong, K. Chen, M. C. Lin, L. Lee, *Organometallics* **2005**, *24*, 4198; h) R. C. J. Atkinson, K. Gerry, V. C. Gibson, N. J. Long, E. L. Marshall, L. J. West, *Organometallics* **2007**, *26*, 316; i) J. Durand, S. Gladiali, G. Erre, E.

Zangrando, B. Milani, *Organometallics* **2007**, *26*, 810; j) N. J. Long, *Angew. Chem. Int. Ed. Engl.* **1995**, *34*, 21; k) Special issue, "50th Anniversary of the Discovery of Ferrocene": R. D. Adams, *J. Organomet. Chem.* **2001**, *637–*639 and references therein.
[4] a) G. Hogarth, M. M. Álvarez-Falcón, *Inorg. Chim. Acta* **2005**, *358*, 1386; b) S. Back, R. A. Gossage, H. Lang, G. van Koten, *Eur. J. Inorg. Chem.* **2000**, 1457; c) H. Lang, S. Köcher, S. Back, G. Rheinwald, G. van Koten, *Organometallics* **2001**, *20*, 1968; d) J. Vicente, M.-T. Chicote, M.-D. Abrisqueta, *Organometallics* **1997**, *16*, 5628; e) T. A. Zevaco, H. Görls, E. Dinjus, *Polyhedron* **1998**, *17*, 613; f) V. W.-W. Yam, K.-L. Cheung, E. C.-C. Cheng, N. Zhu, K.-K. Cheung, *Dalton Trans.* **2003**, 1830; g) J. Vicente, M. T. Chicote, M. M. Alvarez-Flacón, M. D. Abrisqueta, F. J. Hernández, P. G. Jones, *Inorg. Chim. Acta* **2003**, *347*, 67; h) I. R. Whittall, M. G. Humphrey, S. Houbrechts, A. Persoons, D. C. R. Hockless, *Organometallics* **1996**, *15*, 5738; i) J. Vicente, M. T. Chicote, M. D. Abrisqueta, M. C. R. de Arellano, P. G. Jones, M. G. Humphrey, M. P. Cifuentes, M. Samoc, B. Luther-Davis, *Organometallics* **2000**, *19*, 2968.
[5] a) D. A. Edwards, M. F. Mahon, T. J. Paget, *Polyhedron* **2000**, *19*, 757–764; b) H.-M. Gau, C.-C. Schei, L.-K. Liu, L.-H. Luh, *J. Organomet. Chem.* **1992**, *435*, 43; c) T. Güthner, U. Thewalt, *J. Organomet. Chem.* **1989**, *371*, 43; d) X. Meng, H. Hou, G. Li, B. Ye, T. Ge, Y. Fan, Y. Zhu, H. Sakiyama, *J. Organomet. Chem.* **2004**, *689*, 1218; e) H. Hou, L. Li, G. Li, Y. Fan, Y. Zhu, *Inorg. Chem.* **2003**, *42*, 3501; f) Y. Cui, F. Zheng, Y. Qian, J. Huang, *Inorg. Chim. Acta* **2001**, *315*, 220; g) Y. Cui, Y.-T. Qian, J. Huang, *Polyhedron* **2001**, *20*, 1795; h) G. Li, Z. Li, H. Hou, X. Meng, Y. Fan, W. Chen, *J. Mol. Struct.* **2004**, *694*, 179.
[6] T. Y. Orlova, Y. S. Nekrasov, P. V. Petrovskii, M. G. Ezernitskaya, B. V. Lokshin, M. K. Minacheva, L. A. Strunkina, O. L. Lependina, T. V. Magdesieva, S. V. Milovanov, K. P. Butin, *Russ. Chem. Bull.* **1997**, *46*, 1018.
[7] K. Rößler, T. Rüffer, B. Walfort, R. Packheiser, R. Holze, M. Zharnikov, H. Lang, *J. Organomet. Chem.* **2007**, *692*, 1530.
[8] G. A. Koutsantonis, G. C. Iee, C. L. Raston, *J. Chem. Soc., Chem. Commun.* **1994**, 1975.
[9] D. A. Brown, W. Errington, N. J. Fitzpatrick, W. K. Glass, T. J. Kemp, H. Nimir, Á. T. Ryan, *Chem. Commun.* **2002**, 1210.
[10] R. J. Pafford, T. B. Rauchfuss, *Inorg. Chem.* **1998**, *37*, 1974.
[11] R. Claus, Diploma Thesis **2007**, TU Chemnitz, Germany.
[12] Z. Yaokun, W. Zhiqiang, *Polyhedron* **1990**, *9*, 783.
[13] a) J. E. Aguado, S. Canales, M. C. Gimeno, P. G. Jones, A. Laguna, M. D. Villacampa, *Dalton Trans.* **2005**, 3005; b) F. Canales, M. C. Gimeno, P. G. Jones, A. Laguna, C. Sarroca, *Inorg. Chem.* **1997**, *36*, 5206; c) D. T. Hill, G. R. Girard, F. L. McCabe, R. K. Johnson, P. D. Stupik, J. H. Zhang, W. M. Reiff, D. S. Eggleston, *Inorg. Chem.* **1989**, *28*, 3529.
[14] M. C. Etter, *Acc. Chem. Res.* **1990**, *23*, 120.
[15] P. Gilli, V. Bertolasi, B. Ferretti, G. Gilli, *J. Am. Chem. Soc.* **1994**, *116*, 909.
[16] A. Beheshti, W. Clegg, S. H. Dale, R. Hyvadi, *Inorg. Chim. Acta* **2007**, *360*, 2967.
[17] M. O. Sinnokrot, E. F. Valeev, C. D. Sherrill, *J. Am. Chem. Soc.* **2002**, *124*, 10887.
[18] a) A conversion of given electrode potentials to the standard normal hydrogen electrode scale is possible: H. Strehlow, W. Knoche, H. Schneider, *Ber. Bunsenges. Phys. Chem.* **1973**, *77*, 760; b) G. Gritzner, J. Kuta, *Pure Appl. Chem.* **1984**, *56*, 461.
[19] J. Podlaha, P. Štěpnička, I. Císařová, J. Ludvík, *Organometallics* **1996**, *15*, 543.
[20] P. Štěpnička, L. Trojan, J. Kubišta, J. Ludvík, *J. Organomet. Chem.* **2001**, *637–639*, 291.
[21] T. Weidner, K. Rößler, P. Zoufalá, H. Lang, M. Grunze, M. Zharnikov, *J. Electroanal. Chem.* **2008**, *621*, 159.
[22] C. Nataro, A. N. Campbell, M. A. Ferguson, C. D. Incarvito, A. L. Rheingold, *J. Organomet. Chem.* **2003**, *673*, 47.
[23] M. Isobe, S. Kondo, N. Nagasawa, T. Goto, *Chem. Lett.* **1977**, 679.
[24] M. Ciampolni, G. P. Speroni, *Inorg. Chem.* **1966**, *5*, 45.
[25] G. J. Erskine, D. A. Wilson, J. D. McCowan, *J. Organomet. Chem.* **1976**, *114*, 119.
[26] P. M. Druce, B. M. Kingston, M. F. Lappert, T. R. Spalding, R. C. Srivastava, *J. Chem. Soc. A* **1969**, *14*, 2106.
[27] J. Polin, H. Schottenberger, *Org. Synth.* **1996**, *73*, 262.
[28] M. D. Rausch, A. Siegel, *J. Org. Chem.* **1969**, *34*, 1974.
[29] K. C. Dash, H. Schmidbaur, *Chem. Ber.* **1973**, *106*, 1221.
[30] G. M. Sheldrick, *Acta Crystallogr., Sect. A* **1990**, *46*, 467.
[31] A. Altomare, G. Cascarano, C. Giacovazzo, A. Gualardi, *J. Appl. Crystallogr.* **1993**, *26*, 343.
[32] G. M. Sheldrick, *SHELXL-97, Program for Crystal Structure Refinement*, University of Göttingen, Germany, **1997**.
[33] W. Massa, *Kristallstrukturbestimmung*, Teubner Studienbücher, Stuttgart, **1996**.
[34] W. Clegg, *Crystal Structure Determination*, Oxford University, **1998**.

Received: May 26, 2008
Published Online: September 30, 2008

